Article:
Wang, Q, Glover, PWJ orcid.org/0000-0003-1715-5474, Yang, S et al. (3 more authors) (2021) Oil production performance and reservoir damage distribution of miscible CO2 soaking-alternating-gas (CO2-SAG) flooding in low permeability heterogeneous sandstone reservoirs. Journal of Petroleum Science and Engineering. 108741. ISSN 0920-4105

https://doi.org/10.1016/j.petrol.2021.108741

Oil production performance and reservoir damage distribution of miscible CO_2 soaking-alternating-gas (CO_2-SAG) flooding in low permeability heterogeneous sandstone reservoirs

Qian Wang[1*], Jian Shen[1*],Paul W.J. Glover[2], Piroska Lorinczi[2] , Shenglai Yang[3], Hao Chen[3]

1 School of Resources and Geosciences, China University of Mining and Technology, Xuzhou, 221116, China

2 School of Earth and Environment, University of Leeds, Leeds, LS2 9JT, UK

3 School of Petroleum Engineering, China University of Petroleum-Beijing, Beijing 102249, China

*Correspondence: wq5635137@163.com

Abstract: Miscible CO_2-SAG flooding is an enhanced form of CO_2 flooding, which mitigates the inadequate CO_2-crude oil interaction by adding a CO_2 soaking period just after CO_2 breakthrough (BT). The addition of the soaking process results in improvements in the recovery of residual oil during the secondary CO_2 flooding process, which may vary across the reservoir, and lead to differential changes in the distribution of permeability decline and wettability variation due to asphaltene precipitation. In this work, CO_2-SAG and simple miscible CO_2 flooding experiments were carried out at reservoir conditions (90°C, 23 MPa) on low permeability long composite cores with progressively decreasing permeability in the direction of injection. The results show that the overall oil recovery factor (RF) was 72.8% after CO_2-SAG flooding, 11% higher than simple miscible CO_2 flooding (61.8%). The oil RFs of individual core plugs decreased progressively along the core (i.e., with decreases in initial permeabilities). The inadequate interaction occurs more for those cores with low permeability and high residual oil saturation close to the outlet. Consequently, recovery is improved more in lower permeability cores, particularly in medium sized pores of these cores. By contrast, the permeability decline of core plugs after CO_2-SAG flooding was 8-20%, 1.0-4.5% higher than that after simple miscible CO_2 flooding. The permeability decline of the cores close to the injection end showed a slight increase, and continued to decrease along the injection direction after CO_2 flooding. However, the overall decline in core permeability at the injection end was greater than that at the outlet. The soaking process led to a more homogeneous distribution of permeability decline and a greater increase in permeability decline. The distribution of wettability variation was consistent with the distribution of

residual oil saturation after CO_2 flooding. The wettability variation was larger and the cores in middle had the biggest values after SAG flooding.

Keywords: CO_2-SAG flooding, heterogeneous reservoirs, asphaltene precipitation, distribution of residual oil, soaking process, permeability decline.

Introduction

Low-permeability sandstone reservoirs have small pores and throat radii, and have lateral and vertical heterogeneity. The types, distribution, and connectivity of pores and throats are complex and changeable, which makes development difficult. Gas-flooding with CO_2 is an useful and well-understood form of enhanced oil recovery (EOR) which is effective in low-permeability sandstone reservoirs [1]. The CO_2-EOR technique owes its efficacy to four mechanisms; (i) the promotion of oil-swelling, (ii) the reduction of oil viscosity, (iii) the extraction of light-hydrocarbons, and (iv) the reduction of interfacial tension (IFT). Higher efficiencies may be attained if the flooding is carried out at miscible conditions[2-3]. Unfortunately, CO_2-EOR promotes the precipitation of asphaltene, which can cause a significant decline in both the permeability and water wettability of the reservoir[4-5].

Asphaltene is a mixture, which is insoluble in normal alkanes but soluble in aromatic hydrocarbons in crude oil. The dissolution of CO_2 in crude oil or the extraction of light components of crude oil by CO_2 leads to variations in the thermodynamic parameters of the crude oil system and its composition during CO_2 flooding, causing asphaltenes to aggregate into asphaltene solid particles form crude oil in reservoir. Some asphaltene particles are adsorbed onto the internal surfaces of the rock, reducing porosity, permeability and water wettability. Other particles of asphaltene remain mobile. These particles are transported through the rock with the pore fluid, causing pore and pore-throat blockages, and leading to more significant reductions in permeability[6]. Furthermore, due to the differences in the distribution of injected CO_2 in different positions of the reservoir, the CO_2 flooding efficiency and residual oil saturation of the reservoirs at different distances from the injection and production ends are different, resulting in different degrees of damage to reservoirs in different locations. Consequently, the overall efficiency of the CO_2-EOR process is particularly sensitive to the heterogeneity of the reservoir[7-8].
Continuous miscible CO_2 injection provides high oil displacement efficiencies, is simple to implement and is low-cost. Unfortunately, it is associated with premature CO_2 breakthrough (BT) associated with viscous fingering and gravity segregation, which is exacerbated by reservoir heterogeneity. After the CO_2 BT occurs, the efficiency of CO_2 flooding is very low, resulting in a large amount of CO_2 being injected for little extra produced oil. Furthermore, extraction of the light components in the residual oil by CO_2 is effective, and more CO_2 is dissolved in the residual oil, which greatly increases the

precipitation of asphaltenes [9].

The CO_2-SAG flooding process is an EOR method which combines continuous miscible CO_2 flooding with a period of CO_2-soaking, derived from the CO_2 huff-and-puff processes[10]. It is implemented in 3 phases. The first phase involves the continual injection of CO_2 at miscible conditions until CO_2 breakthough(BT). In this phase, oil is displaced as efficiently as during the pre-breakthrough phase of the simple miscible CO_2 flooding process, to which it is, of course, identical. In phase 2, both the injector and producer are shut in for a pre-determined CO_2-soaking period. During this time the injected CO_2 has the opportunity to diffuse into reservoir fluids that hitherto were not in contact with CO_2 (as a result of the viscous fingering and the consequent early CO_2 breakthrough). The oil expands and its viscosity decreases considerably during the soaking period as the partial pressure of CO_2 in the residual oil rises. The larger oil volume and lower viscosity both allow the oil to enter the former CO_2 flow pathways and CO_2 breakthrough channels[11-12]. The soaking period provides the extra time the CO_2 needs to interact fully with the residual oil, substantially increasing CO_2 sweep and displacement efficiency in the subsequent secondary CO_2 flooding, which is the third phase of the process. The resulting higher CO_2 utilization efficiency results in lower injection costs compared with simple miscible CO_2 flooding. The combination of these effects allows the subsequent secondary CO_2 flooding to displace and recover more residual oil[13-14].

The soaking process produces different degrees of improvement in oil production in different locations of reservoirs which have heterogeneous pore size and permeability distributions. Reservoir heterogeneity also affects the distribution and amount of reservoir damage after flooding[8,15]. Consequently, it is necessary to evaluate the effect of the CO_2-SAG process for oil recovery improvement and reservoir damage limitation. Since the results of the process are sensitive to reservoir heterogeneity, its advantages and disadvantages need to be evaluated in different locations with different pore-sizes and permeabilities in a way in which the results can be compared directly with the results obtained from simple miscible CO_2 flooding.

Regrettably, only a few core-flooding experiments studying the technical benefits and significant

potential of SAG injection have previously been carried out and reported in the literature[10-14]. The studies, however, are informative enough to allow us to target several important variable parameters and processes which would need to be studied. These include CO_2 injection pressure, injection mass/volume flow rate, the CO_2 soaking period, pre-water flooding, and the pore-throat structure of cores at the microscopic level[13]. Until now comparison of the distribution of the improvement in oil production and reservoir damage at different locations in heterogeneous reservoirs after CO_2-SAG flooding and miscible CO_2 flooding has not been studied.

In this paper, the process of the reservoir condition miscible CO_2-SAG process and simple miscible CO_2 flooding were conducted on two similar groups of low permeability long composite cores (of 36 cm), with decreasing permeability along the injection direction. This paper examines the efficacy of the miscible CO_2-SAG flooding process with particular attention paid to (i) the displacement characteristics, (ii) the distribution of improved oil production, (iii) the difference in permeability damage, (iv) and the variation in wettability by asphaltene precipitation, adsorption and transport, all for different pore-size and permeability core plugs representing different areas within a heterogeneous reservoir. Each measurement and effect has been compared directly with the results obtained from simple miscible CO_2 flooding. The results provide experimental and theoretical support for accurate assessment of residual oil saturation and reservoir damage at different locations after CO_2 injection by different methods, which is the basis for selecting subsequent measures for EOR.

Methodology

Materials

A representative oil sample was obtained from block H of Jilin Oilfield, which is located in the Jilin province section of the Songliao Basin in the northeast China. The block H is a typical low-permeability heterogeneous oil reservoir deposited in a delta front environment with a depth of 2000 m to 2500 m and a thickness of 3 m to 18 m. The synthetic live oil used in the experiments was prepared in the laboratory based on the compositional analysis of the crude oil measured using a high-temperature gas chromatograph (HTGC) (Table 1). The content of *n*-C_5 insoluble asphaltene was 3.18 wt% (ASTM

D2007-03 standard method). The minimum miscible pressure (MMP) of the crude oil-CO_2 system at 90±0.1°C was 20.6±0.4 MPa, as measured using a slim-tube apparatus[13]. The relationship between CO_2 concentration in crude oil and asphaltene precipitation (Figure 1) can be predicted based on the Flory-Huggins model [8,16], the difference between the experimentally measured value and the predicted value is less than 5%. The pressure–volume–temperature (PVT, Ruska,USA) tests were conducted to obtain the pressure at which asphaltene begins to precipitate in crude oil at reservoir conditions, which is 11.4 MPa, and the solubility of CO_2 in the crude oil at 23 MPa and 90 °C, which is 69.4 mol%. It shows that the asphaltenes in crude oil have almost completely precipitated out before CO2 reaches the maximum dissolved concentration in crude oil under formation conditions in Figure 1. The purity of CO_2 used in this study was 99.99%. The two types of brine (ordinary brine and brine containing Mn^{2+}), which were used in experiments, were prepared according to the composition of formation water (Table 2). The brine containing Mn^{2+} is used to shield the water signal during nuclear magnetic resonance (NMR) tests to obtain the oil distribution in the core [17].

Table 1. Basic physical properties of live oil together with its compositional analysis (n-C5 insoluble asphaltene content =3.18 wt%).

Property			**Value**		
Density (g/cm^3)			0.731±0.002 (90°C)		
Viscosity (cP)			2.11±0.04 (90°C)		
Solution gas-oil ratio (m^3/m^3)			44.7		
Bubble point pressure (MPa)			6.95		
Composition					
Carbon number	**wt%**	**Carbon number**	**wt%**	**Carbon number**	**wt%**
CO_2	0.053	C_9	4.640	C_{21}	2.16
N_2	0.422	C_{10}	4.531	C_{22}	2.304
C_1	1.741	C_{11}	3.947	C_{23}	2.104
C_2	1.126	C_{12}	3.615	C_{24}	2.088
C_3	0.998	C_{13}	3.261	C_{25}	1.948
iC$_4$	0.178	C_{14}	2.908	C_{26}	1.872
nC$_4$	0.525	C_{15}	2.633	C_{27}	1.896
iC$_5$	0.942	C_{16}	3.615	C_{28}	1.766
nC$_5$	0.353	C_{17}	3.567	C_{29}	1.882
C_6	1.365	C_{18}	3.222	C_{30+}	26.363
C_7	2.52	C_{19}	2.484	**Total**	**100**

C_8	4.409	C_{20}	2.563

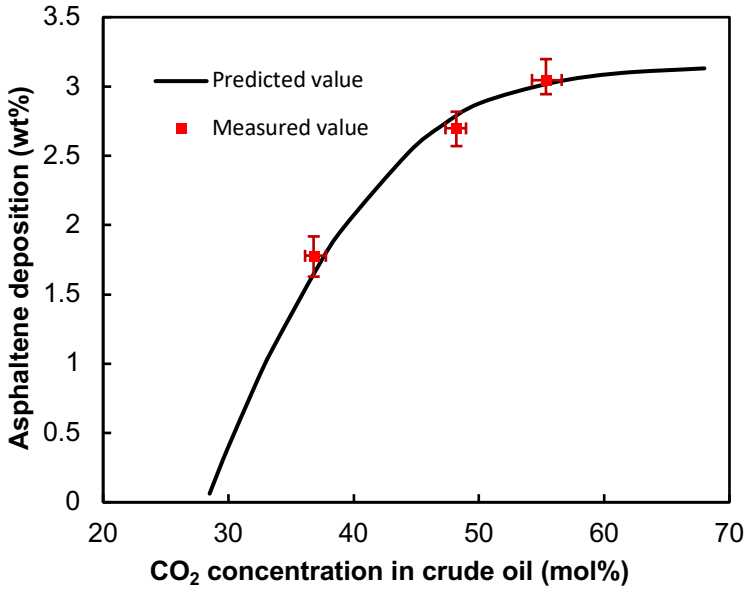

Figure 1. Effect of CO_2 on the amount of asphaltene deposition (wt%) at P=23±0.02MPa and T=90±0.1°C.

Table 2. Physicochemical properties of the reservoir brine.

Item	Value
Density (g/cm^3)	1.005
Viscosity at 25°C (cP)	1.02
pH	7.04
K^+ (mg/L)	1473
Na^+ (mg/L)	3546
Ca^{2+} (mg/L)	116
Mg^{2+} (mg/L)	33
Cl^- (mg/L)	5261
SO_4^{2-} (mg/L)	1288
HCO_3^- (mg/L)	1559
TDS (mg/L)	13276

TDS = Total dissolved solids.

The cores used in the experiments were collected from the reservoir with a depth of 2252-2560 m in block H. The reservoir permeability gradually decreases from injection well to production well, and the

permeability of the reservoir near the injection well is about 3 times the permeability of the reservoir near the production well, therefore, 12 homogeneous cores were selected to form a long composite core to simulate a reservoir with the above characteristics. All the cores are divided into two equal parts to form two groups of long composite cores with similar physical properties for CO_2 flooding and CO_2-SAG flooding experiments. The length of each core is close to 3 cm (±0.2 cm), and the measured gas permeability and porosity of all cores are shown in Table 3. It is worth noting that before the cores are cut, the left end and the right end of the cores were marked separately, the short cores were inserted in the core holder in the same direction to make sure that the fluid is always injected from the left end of the cores during flooding (Figure 2). X-ray diffraction tests (XRD, Model: D8 Focus, Bruker, MA, USA) were performed on the fragments from the cores, and the average value of each mineral content was obtained as shown in Table 4.

Table 3. Basic parameters of the core samples.

Core number	Length (cm)	Diameter (cm)	Permeability (mD)	Porosity (%)	Core number	Length (cm)	Diameter (cm)	Permeability (mD)	Porosity (%)
1-1	3.14	2.52	4.326	18.20	2-1	3.10	2.52	4.341	18.16
1-2	2.93	2.52	4.298	18.10	2-2	3.05	2.51	4.333	18.12
1-3	3.06	2.53	3.717	16.43	2-3	3.09	2.52	3.728	16.55
1-4	3.02	2.52	3.503	18.02	2-4	2.96	2.51	3.483	17.98
1-5	3.10	2.52	3.217	17.07	2-5	3.15	2.52	3.179	16.97
1-6	3.05	2.52	2.896	16.25	2-6	3.03	2.53	2.853	16.18
1-7	3.20	2.52	2.631	15.92	2-7	3.15	2.52	2.610	15.86
1-8	3.05	2.53	2.348	15.24	2-8	3.07	2.52	2.344	15.14
1-9	3.13	2.53	1.962	16.39	2-9	3.09	2.53	1.947	16.57
1-10	2.88	2.52	1.783	15.47	2-10	3.00	2.52	1.791	15.56
1-11	2.97	2.51	1.769	15.79	2-11	2.92	2.52	1.776	15.87
1-12	3.08	2.52	1.654	14.49	2-12	3.18	2.52	1.663	14.61

Table 4. Types and average content of mineral in the cores.

Mineral	Content (wt%)
Quartz	36.1
K-feldspar	17.4
Plagioclase	25.7
Calcite	7.5
Dolomite	4.7
Clay minerals	6.8
Others	1.8

Core-flooding tests

The schematic diagram of the high-pressure apparatus used for core-flooding experiments is shown in Figure 2. Brine, live oil, brine with $MnCl_2$ (Mn^{2+}, 15000 mg/dm^3), and CO_2 were delivered separately to the core from four high pressure cylinders (Hongda, China; P=80 MPa; T=130°C). A dual ISCO syringe pump was used to control injection from the high pressure cylinders to the core in the core holder. The core holder is 50 cm long with 3 pressure test ports (Hongda, China; P=40 MPa; T=110°C). A pump was used to maintain confining pressure, and another pump and a back pressure valve were used together to regulate and maintain the back pressure. The cylinders and core holder were placed in the constant temperature oven (Hongda, China; T=150.0±0.1°C) with the temperature being regulated within ±0.1°C by the temperature controller. The produced brine, oil and gas were collected and

quantified by a gas-liquid cyclone separator and a mass flow meter. Flow data and pressure were logged by computer during the experiments.

The core-flooding procedure was carried out as follows:

1. The constant temperature oven was raised to 90±0.1°C and held at that temperature for 24 hours. The individual core plugs were inserted into the core holder, ensuring that the permeability of the core plugs composing the long composite core gradually increased from the highest permeability at the injector-end to the lowest permeability at the producer-end. The composite core was then cleaned and dried, evacuated and saturated with ordinary brine. Once the saturation had taken place, the composite core was unloaded and dismantled into individual core plugs. The transverse relaxation time (T_2) spectrum of the brine in each core plug at initial water-saturated conditions was measured using a nuclear magnetic resonance spectrometer (NMR, Mini-MR, Niumag, Suzhou, China). The T_2 and magnetization of the hydrogen nuclei of the fluid in all core pores are detected and recorded in the T_2 spectrum during the MNR tests. Since the amplitude of transverse magnetization is proportional to the number of hydrogen nuclei and the value of T_2 is determined by the size of the pore space in which the hydrogen nuclei are located. Consequently, the T_2 spectrum can represent the distribution of fluid in the core pores.The core plugs were then dried and reinserted into the core holder again in the same order as before. The composite core was evacuated and saturated with the $MnCl_2$-enriched brine. Crude oil was injected into the composite core to displace water, imitating the initial oil emplacement. The oil injection was stopped after 30 hydrocarbon pore volumes (HCPV) in order to achieve an initial oil saturation (S_{oi}) and connate water saturation (S_{wc}). The composite core was unloaded and dismantled into individual core plugs once again. Each of the core plugs was remeasured using the NMR apparatus to obtain the T_2 spectrum of oil in each core. After that all the cores were reinserted into the core holder, again in the same order, and another 5 HCPV crude oil was injected into the composite core. The core holder was left undisturbed for at least 24 hours to attain an equilibrium condition at 90±0.1 °C and 23±0.02 MPa.

2. In each flooding test, a constant flow rate of 0.02±0.0005 cm^3/min of CO_2 was injected into the core-holder to displace the crude oil. The pressure at the outlet of the core holder was maintained at 23±0.02 MPa. For simple miscible CO_2 flooding, the core-flood was stopped when no more oil evolved from the long composite core during CO_2 flooding. However, for CO_2-SAG flooding, the core-flood was stopped when CO_2 breakthrough occurred. The valves at the inlet and outlet of the core holder were closed during the CO_2 soaking stage. After the soaking stage had finished, the valves were opened and CO_2 was once again injected into the core holder to displace the crude oil after the pressures in the core holder had stabilized, until no more crude oil was produced.

3. The volumes of injected and produced fluid, as well as the injection and production pressures were recorded continuously throughout the entire flooding experiment. The gas in the core holder was released slowly by gradually reducing the pressure, and the volume of gas was measured after flooding. Then the cores were taken out and re-tested by NMR to obtain the distribution of the residual oil in each core after flooding. The produced oil was collected during each core-flood test, and the asphaltene content in the produced oil was analysed.

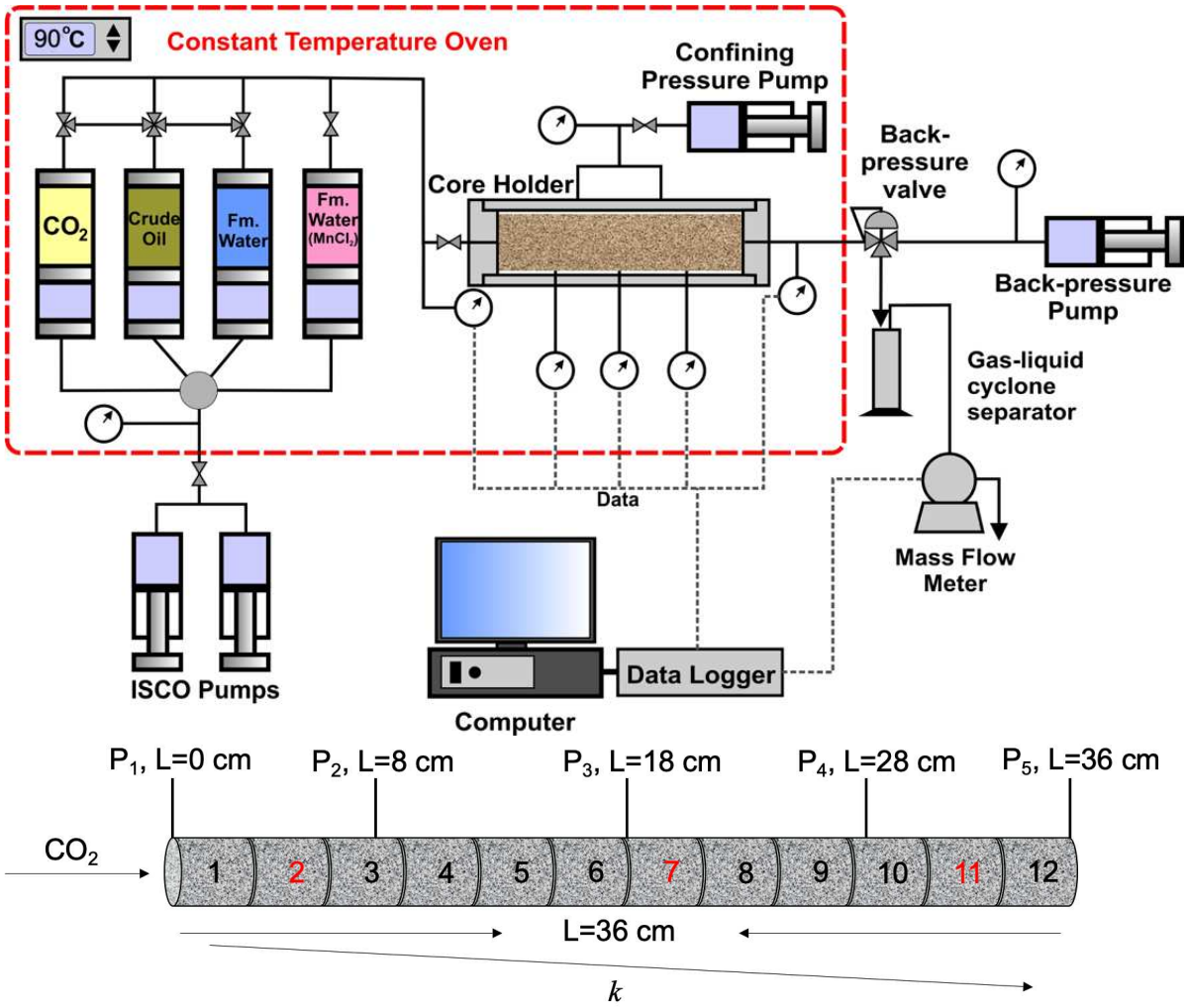

Figure 2. Schematic diagrams of (top) the core-flood apparatus, and (bottom) the components of the long composite core showing the positions of the fluid pressure transducers. The core plugs labelled in red represent those which were subjected to an enhanced set of post-flooding tests.

Post-flooding tests

Asphaltene is not soluble in alkanes but dissolves readily in aromatic solvents. Consequently, cleaning of the core with *n*-heptane[8] using a Soxhlet extractor (SXT-02, Shanghai Pingxuan Scientific Instrument CO., Ltd., China) can be used to remove all organic components from the core plugs except asphaltene. The core plugs were then dried and their porosities and gas permeabilities were measured. Since the *n*-heptane Soxhlet extraction process left asphaltene in the core, the measured porosities and gas permeabilities are those which are affected by asphaltene precipitation. Subsequently, the cores were aged by soaking in synthetic brine for 24 hours in order to minimize the effect of using saturated

oil on wettability variations. The cores were then saturated with ordinary brine once again and subjected to another NMR spectrometer measurement in order to obtain the T_2 spectrum of the brine distribution with asphaltene in place. The cores were cleaned with alternating floods of toluene and methanol to remove the asphaltene, before being dried. Finally, the cores were subjected to porosity and gas permeability measurements three times in order to obtain a mean value (uncertainties <0.4%).

Results and Discussion

Differential pressures (ΔP)

Figures 3, 4 and 5 show the differential pressures of the four sections of core (*L*=0-8 cm, *L*=8-18 cm, *L*=18-28 cm, *L*=28-36 cm). Taking Figure 3, the differential pressures increased initially due to the combined effects of the strong flow resistance of the two-phase flow and the continuous CO_2 injection. The differential pressures decreased subsequently before the CO_2 BT in the two flooding processes, which was due to the reduction of crude oil viscosity caused by CO_2 dissolution and the continuous advancement of the displacement front towards the outlet[18]. When CO_2 BT occurred (0.625 PV) and the previous CO_2 flow paths or CO_2 BT channels formed in the long composite core, the differential pressures drop rapidly. It should be noted, that in the period between about 0.5 PV and 0.625 PV injection, the portion of the core proximal to injection (*L* = 0-28 cm) experiences the faster pressure reduction due to channelized flow at the same time as the distal end (28-36 cm) is still experiencing a slight pressure reduction solely due to CO_2-mediated viscosity reduction. With the CO_2 continuing to be injected into the composite core, the crude oil is continuously driven out; the larger the CO_2 BT channels, the smaller the differential pressures[19]. When no oil was produced at the outlet, the overall differential pressures difference was the least.

During the miscible CO_2-SAG flooding, after the soaking process, the fluid redistribution in the core reached a new balance[10], CO_2 was continuously injected to displace oil (secondary CO_2 flooding), and the differential pressures rose rapidly to a peak, this may be due to the fact that the amount of CO_2 dissolved in crude oil is relatively large compared to the first flooding, and the amount of CO_2 consumed due to the CO_2 dissolution into the oil is small. The rate of increase of gas-oil ratio (GOR) value at the first CO_2 BT is less than that at the second CO_2 BT, ΔP has a little larger sudden change amplitude at

the first CO_2 BT. Both the maximum differential pressures and the effective duration of the secondary flooding were less and shorter than those of the first flooding, respectively. This observation is associated with (i) the viscosity of the crude oil having been decreased greatly by CO_2 solution during the secondary flooding, and (ii) the CO_2 saturation in the core being already high from the primary flooding. These two factors conspire to make the displacement resistance small, and ensure that the duration of the secondary CO_2 flood is smaller. The time of the second CO_2 BT determines the oil production improvement effect of SAG flooding. Although it comes more quickly with little CO_2 injection than the first CO_2 BT, it effectively prolongs the high-efficiency stage of CO_2 flooding. At the end of the flooding, when the final differential pressures were stabilized, the pressure difference values were smaller than that of the simple miscible CO_2 flooding, primarily because the oil saturation in the core was smaller than that after the CO_2 flooding.

The distribution of the pressure difference ΔP along the cores during flooding is shown in Figure 4. At the beginning of CO_2 injection (0.019PV, CO_2 flooding, 0.015PV, CO_2-SAG flooding), CO_2 in the pores at inlet continues to accumulate with the continuous injection of CO_2, the fluid pressure in the pores increases, and ΔP gradually increases at inlet. With the injection of CO_2 and the advancement of the displacement front, the differential pressures between the four pressure points (P1, P2, P3, P4) and the output face of the core (P5) gradually decreases before the CO_2 BT in the two flooding processes. This is due to the fact that oil saturation in this part of the core gradually decreases, the injected CO_2 gradually forming a continuous phase, and the relative permeability of CO_2 increasing, resulting in the decrease in seepage resistance and the requirement for smaller pressure differences[20]. The pressure differences between P1, P2, P3, P4 and P5 are close and reach the minimum values at the end of flooding, indicating that the CO_2 channel has formed and the CO_2 in the cores has formed a continuous phase.

In all scenarios the outlet part of the long composite core (L=28-36 cm) experiences a high pressure difference because this part of the core has a high residual oil saturation. We express the difference across this output 8 cm of the composite core as a percentage of the pressure drop across the whole core and give it the symbol R_Δ. This output section percentage pressure drop gradually increases during flooding for both simple miscible CO_2 flooding and miscible CO_2-SAG flooding, as shown in Figure 5.

During simple miscible CO_2 flooding, R_Δ increases up to and beyond CO_2 BT. For the miscible CO_2-SAG, the value of R_Δ increases in the same way as for the simple miscible flooding. However, the suspension of flooding and instigation of a soaking period leads to a decrease in R_Δ, before the steady increase resumes during the secondary injection phase. This shows that the R_Δ acting on the CO_2 flooding power in the cores near the inlet increases due to the soaking process, and the R_Δ at outlet is reduced, which is beneficial to EOR. As the secondary CO_2 flooding progressed, the R_Δ at outlet continued to increase. This behavior is a clear indication that production wells sited in low permeability rocks, which may be encountered in heterogeneous reservoirs, will cause problems for optimal hydrocarbon recovery, irrespective of whether miscible CO_2 flooding or miscible CO_2-SAG flooding is used. Indeed, our results (Figure 5) show that is marginally more sensitive to this problem.

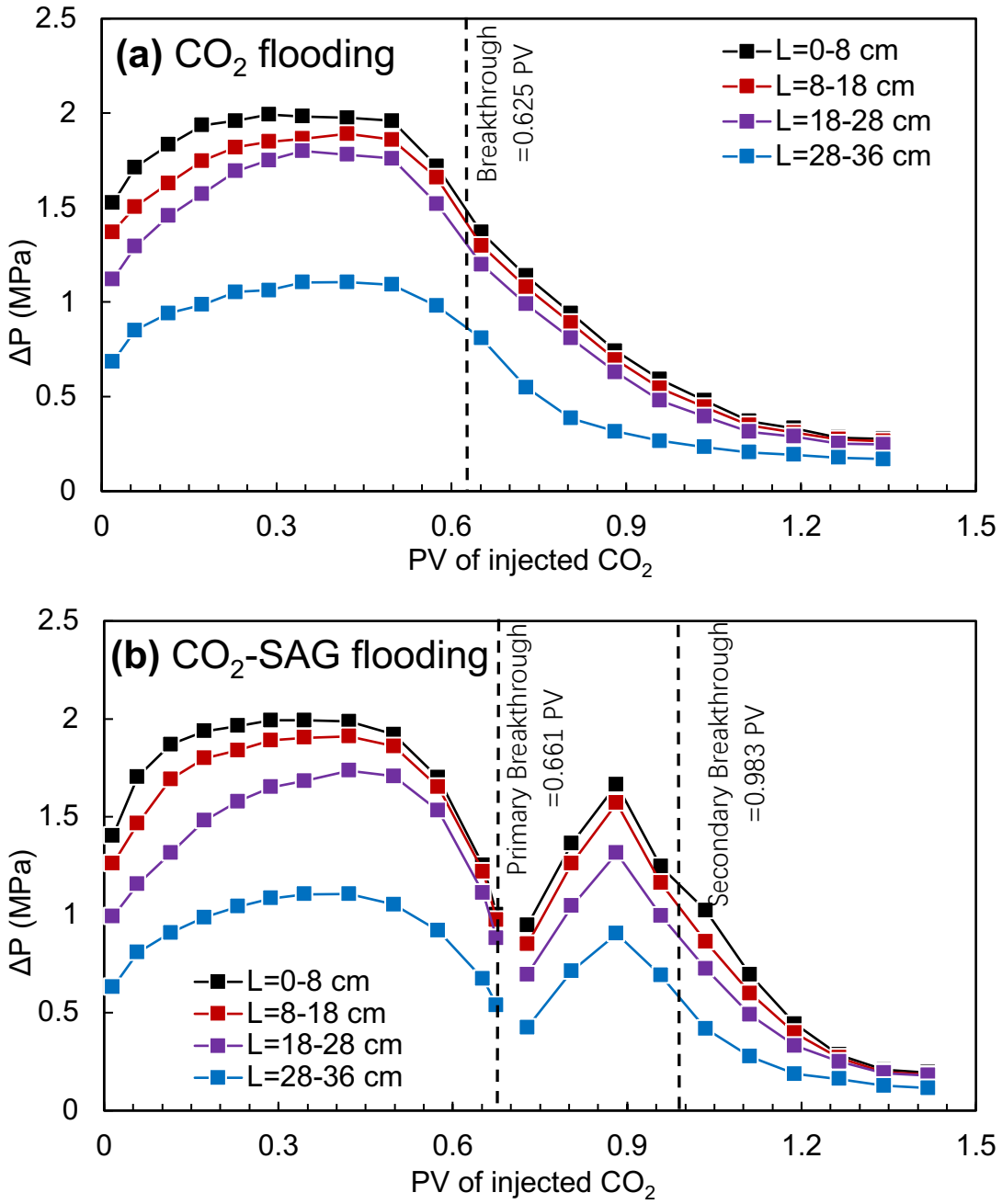

Figure 3. Measured differential pressure (ΔP) between 4 portions of the composite core during (a) simple miscible CO_2, and (b) miscible CO_2-SAG flooding.

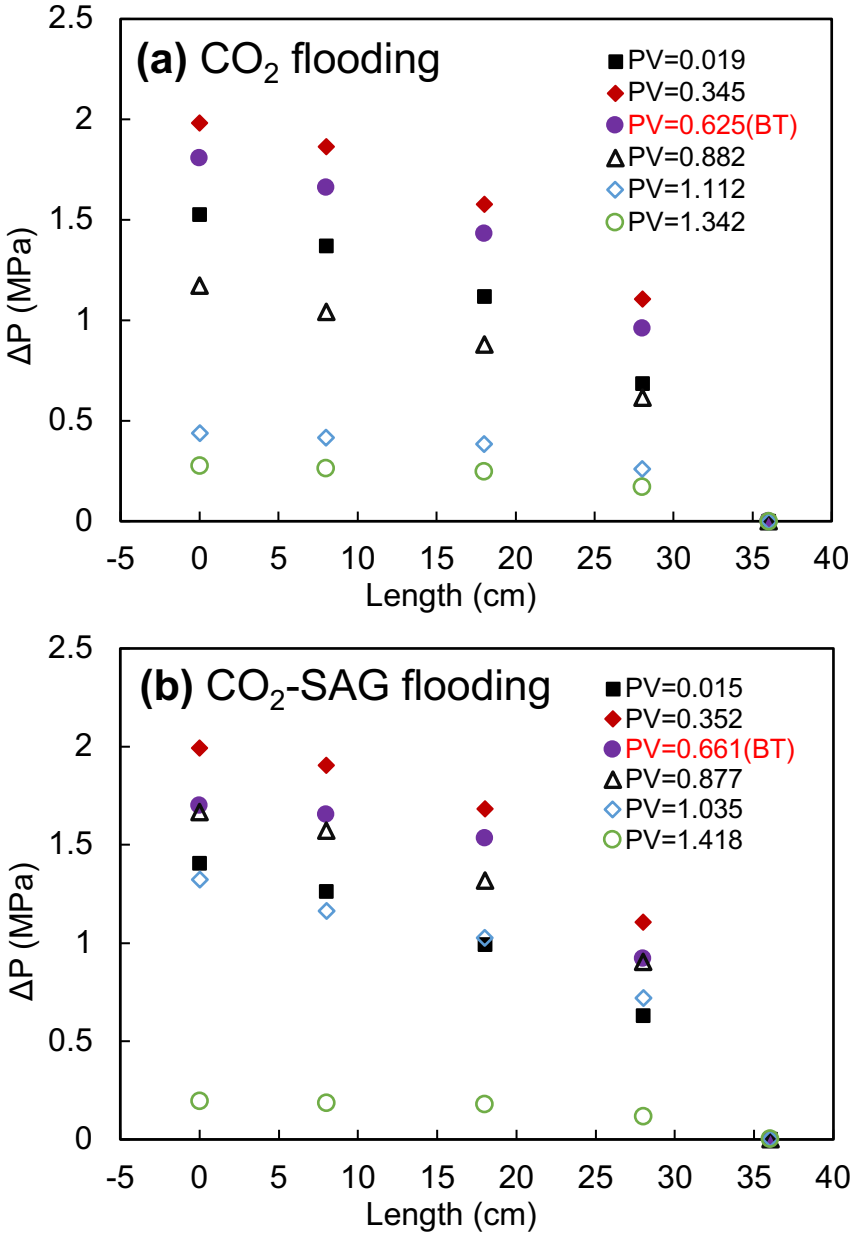

Figure 4. The distribution of ΔP along the cores during flooding.

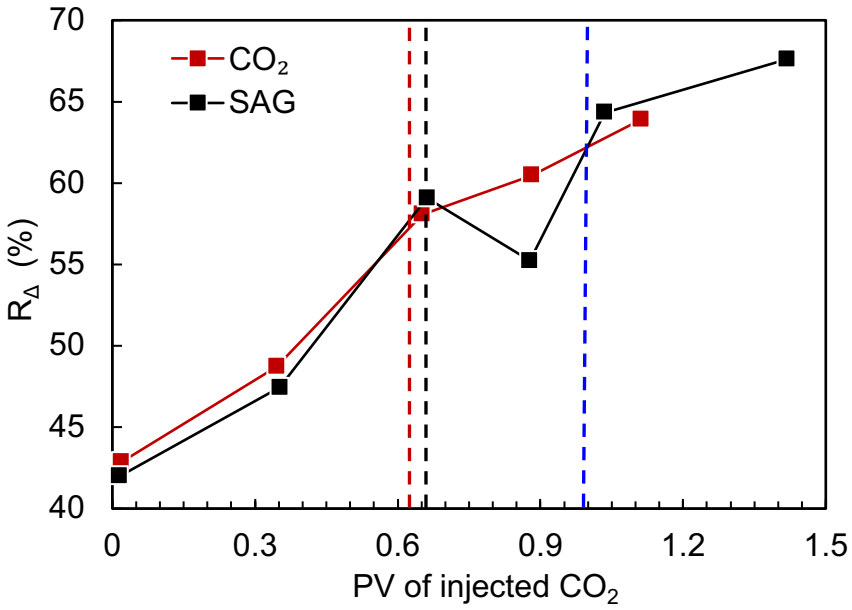

Figure 5. The proportion of ΔP of the 8 cm long composite core at the outlet to the total ΔP (R_Δ). The vertical dashed lines represent the CO_2 BT for the simple miscible CO_2 flooding process (black), and the primary and secondary BTs from the CO_2-SAG process (black and blue, respectively).

Pressure decay during the CO_2-soaking process

During the soaking process the CO_2 that has been placed in breakthrough channels and other accessible pore spaces dissolves gradually in the neighboring crude oil, which results in a decline in the CO_2 pressure in the core[21], as shown in Figure 6. In this figure, the gas pressure is the arithmetic mean of gas pressures measured at five points along the composite core. During the soaking process it can be assumed that there is good gas connectivity between the inlet and outlet through channels resulting from the initial miscible gas flooding, which were formed up to CO_2 breakthrough. Hence, differential pressures are relatively small, and the pressure values at each of the 5 measurement points quickly reaches a steady-state value at about 5 MPa below the pressure at the start of the soaking process[10].

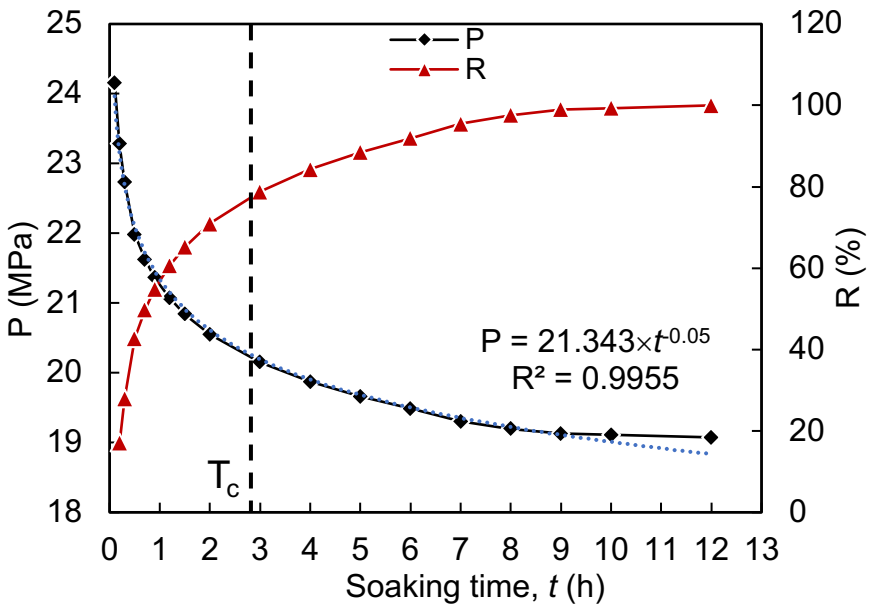

Figure 6. (P) Arithmetic mean gas pressure in the core plugs as a function of soaking time, shown together with a best-fit power law and its equation and coefficient of determination, and (R) the percentage of pressure decay with respect to the pressures at the start of soaking and that when a steady-state has been attained, again as a function of the soaking time. The critical time according to our definition (please see text) is shown as a vertical dashed line.

The measured arithmetic mean gas pressure inside the core declines rapidly, reaching a steady value after about 12 hours (Figure 6). The decline can be fitted by a power-law, with an exponent of -0.05. We expect that this relationship arises from the interplay between (i) the process of gas dissolution proximal to the gas phase, where dissolution of gas in oil is controlled by the amount of gas already dissolved in the oil, and (ii) the diffusion of gas within the oil from the proximal region to deeper in the oil phase. Consequently, the process of dissolution becomes steadily less efficient as more gas dissolves in the oil occupying a particular pore space until a steady-state is attained[22]. The cores were immersed in brine and aged before the experiments, which makes the cores water-wettability. The crude oil is a non-wetting phase, which is distributed in the center of the relatively large pores and throats of cores. During the flooding process, the injected CO_2 is also a non-wetting phase, preferentially contacting the crude oil in the center of the large pores and throats rather than brine. We hypothesized that the initial rapid decay would be due to gas dissolution in oil that is in direct contact with the CO_2, while the later decay would depend on gas diffusion within the oil[13]. The relatively slow process of gas diffusion in

oil may account for the observation in Figure 6 that the gas pressure at large values of soaking time is larger than predicted by the power-law fit. The molecular diffusion coefficient for oil of the viscosity used in this work can be calculated quickly and easily by using the relationship developed by Ssebadduka et al. (2020), and is $(94.7\pm13.2)\times10^{-9}$ m^2/s[23], at the same time the oil swelling factor and gas dissolution are evaluated. If the soaking time had been continued further, it may have been possible to correlate the rate of long-time decline to this diffusion coefficient. However, such a calculation would need to take into account that gas diffusion through oil in small pores and between pores with small pore throats will be hindered by the lack of connectivity of the oil that is imposed by the rock matrix.

Furthermore, the fluid in small pores is more likely to be brine because the rock is strongly water-wet. The CO_2 will also dissolve in water that is present as an irreducible phase. However, the solubility of CO_2 in brine is lower than that of CO_2 in crude oil under the same temperature and pressure conditions due to salting out effect. A long CO_2 soaking time will result in CO_2 starting to dissolve in the brine as well as in the oil. This results in a reduction in the water viscosity allowing it to become mobile. Such newly mobile water is likely to be displaced by post-soak CO_2 flooding. The efficacy of oil production may be reduced as the newly mobile water may impede oil production and increase the production cost of the oil field [24]. Consequently, we may recognize an optimal soaking time (T_c) which takes advantage of CO_2 dissolution in oil allowing the oil to swell and become more mobile, when the pressure decays quickly, while avoiding the increased mobility of water which occurs at longer soaking times, which is associated with later slow pressure decay. This T_c is a turning point of pressure decay rate, which means that there is a big difference in pressure decay rate before and after this point. Only the rapid decay stage of pressure is retained to save time and improve the efficiency of CO_2-SAG flooding, the soaking stage is finished and the secondary CO_2 displacement is started to avoid the slow pressure decay stage after T_c.

In Figure 6 the pressure decays by 57.6% of the total pressure drop during soaking process in the first hour, 70.8% in the first two hours, and 78.8% in the first three hours. The optimal soaking time can be defined in a number of different ways and may differ from one reservoir to another. In our case an T_c occurs when the pressure decay rate becomes less than 0.4 MPa/h, which occurs after approximately 3

hours. The decay pressure is more than 75% at this point, which means enough CO_2 dissolved into the crude oil and enough interaction time with the crude oil. It should be noted that our criterion for T_c is likely not to apply to all reservoirs. A better alternative would be to adjust the value of T_c to optimize ultimate oil recovery factor, but this would require a large suite of core-flooding tests to be carried out.

The length of the core is also a factor. Both the pressure decay rate and the T_c value (as we have defined it) are shorter for the soaking process for SAG flooding of short cores (L<7 cm) compared to long composite cores[13]. This is expected to arise from the significantly different distribution of injected CO_2 and residual oil at the beginning of the soaking process in the larger-scale heterogeneous porous media, resulting in a longer period being required for the fluid distribution in the pores to reach new equilibrium. Consequently, T_c varies with scale, such that the T_c value in the actual oil field production process is expected to be larger than that during core-flooding experiments.

Oil recovery and produced fluid

Table 5 shows the crude oil RFs and cumulative CO_2 to oil exchange ratio (the volume ratio of produced oil and injected CO_2, R_e, the volume of CO_2 was the volume at formation conditions) of the two flooding experiments. The two flooding experiments achieved similar oil production before the CO_2 BT. The simple miscible CO_2 flooding produced an increase in oil RF by 8.1% of oil originally in place (OOIP), from 53.7% to 61.8% after breakthrough. By contrast, the post-soaking flooding phase of the CO_2-SAG process increased the recovery factor by 20.6% of OOIP, from 52.2% to 72.8%. The estimated ultimate recovery (EUR) for the CO_2-SAG process was 11% of OOIP greater than that for the simple miscible CO_2 process, which is a significant increase when represented in financial terms.

The cumulative CO_2 to oil exchange ratio of the secondary CO_2 flooding was twice that of the continuous CO_2 flooding after the CO_2 BT, due entirely to the soaking process. Although the final cumulative CO_2 to oil exchange ratio of CO_2-SAG flooding was slightly higher than that of simple miscible CO_2 flooding, the overall effective CO_2 flooding process was longer, which increases the upper limit of recoverable oil RF.

Table 5. The crude oil RFs and cumulative CO_2 to oil exchange ratio of the two flooding experiments.

Flooding method	Oil RF at CO_2 BT (%)	Cumulative R_e at CO_2 BT (cm^3/cm^3)	Cumulative R_e after CO_2 BT (cm^3/cm^3)	Final oil RF (%)	Final cumulative R_e after CO_2 BT (cm^3/cm^3)
simple CO_2	53.7	0.54	0.082	61.8	0.322
CO_2-SAG	52.2	0.52	0.167	72.8	0.341

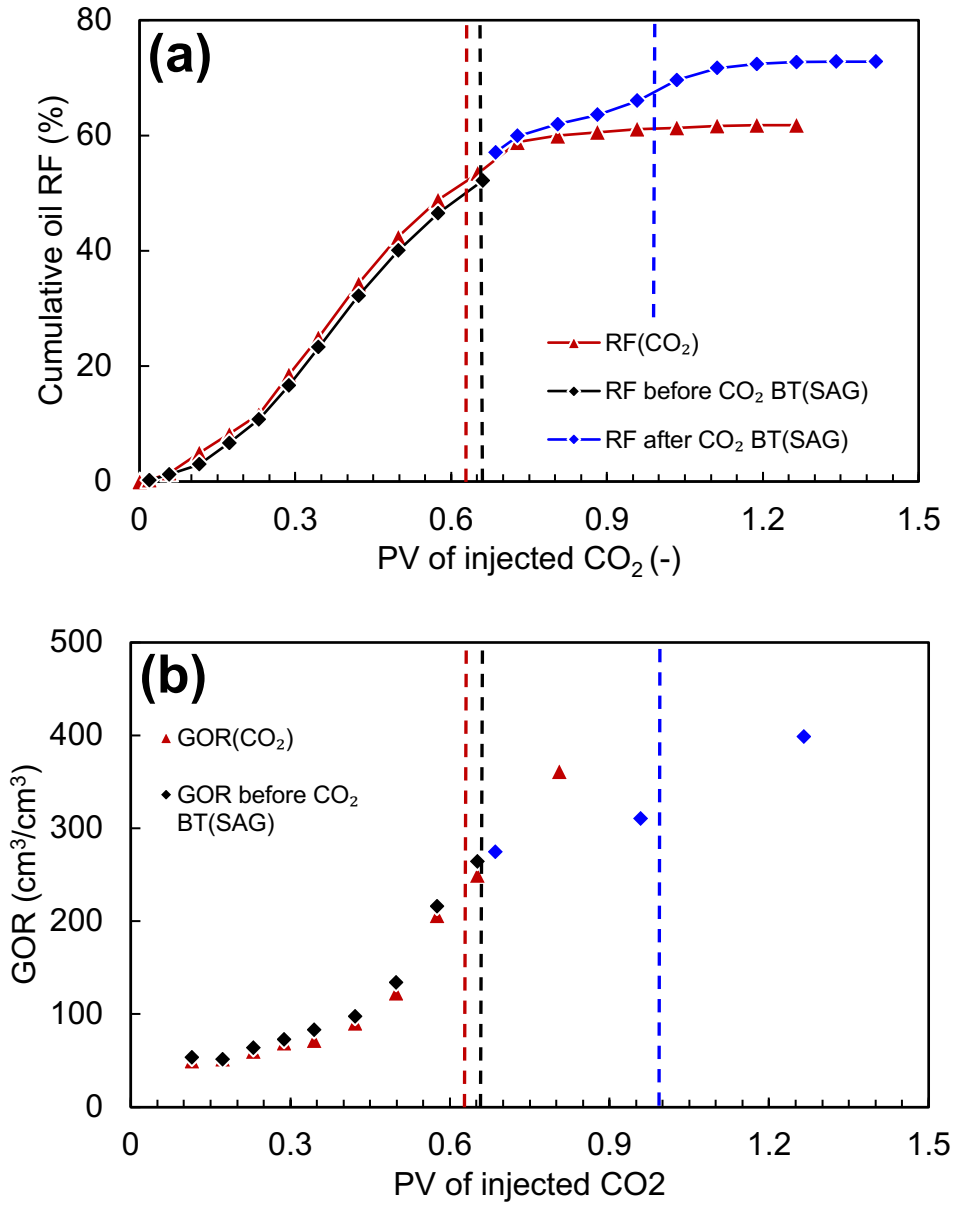

Figure 7. (a) Cumulative crude oil recovery factor, and (b) gas-oil ratio (GOR) as a function of pore volumes of injected CO_2 during flooding for simple miscible CO_2 flooding (red), pre-soak (pre-breakthrough) miscible CO_2-SAG flooding (black), and post-soak secondary miscible CO_2-SAG flooding (blue). The vertical dashed lines represent the CO_2 BT for the simple miscible CO_2 flooding process

(black), and the primary and secondary BTs from the CO_2-SAG process (black and blue, respectively).

The cumulative crude oil recovery factor and gas-oil ratio (GOR) of the fluids produced during CO_2 injection are shown in Figure 7. During the continuous miscible CO_2 flooding, the cumulative oil RF (red line) increased rapidly before the CO_2 BT, and the GOR slowly increased. The produced gas was mainly the gas dissolved in the crude oil (the GOR was close to the original dissolved GOR) before 0.3PV CO_2 was injected, and subsequently the injected CO_2 was produced from the outlet together with associated oil production, whereupon the GOR increased rapidly. After CO_2 BT, there was very little oil production. The extraction of light components in crude oil by CO_2 had an impact on the improvement of crude oil production. The efficiency of CO_2 flooding was very low at this stage, and the GOR accelerated[25].

The CO_2 to oil exchange ratio R_e for both flooding processes is shown in Figure 8a. This ratio is defined as the ratio of the volume of CO_2 injected to the oil produced at any given time, and consequently is expected to contain a time delay, representing the CO_2 flooding efficiency. Both processes exhibit the same pattern before breakthrough, as would be expected. The efficiency of oil displacement by CO_2 increases slowly and reaches a maximum before CO_2 BT, dropping again until CO_2 BT is attained. After CO_2 BT, the CO_2 to oil exchange ratio initially drops further for both processes. However, while the curve for the simple miscible CO_2 process continues to decrease to values extremely close to zero, which is consistent with the extremely high GOR at this stage, the CO_2-SAG process exhibits a second peak, indicating a revival in the efficiency of expelling oil by the secondary gas flooding, after which the CO_2 to oil exchange ratio decreases once more, ultimately also declining to levels very close to zero.

The initial injected CO_2 results in an increase of fluid pressure in the core, whilst also continuously dissolving in the crude oil. As this occurs, the displacement front advances and crude oil is driven out of the core. Up to about 0.4 PV injected, oil is produced by simple displacement. During this displacement some of the CO_2 dissolves in the oil. The dissolution has two competing effects; one to reduce the amount of CO_2 available to displace the oil, the other to decrease the viscosity of the oil making it easier to produce. However, as the injection of CO_2 progresses, the oil at the CO_2/oil interface

becomes saturated with CO_2 which curtails the dissolution process[26]. During this period the CO_2 to oil exchange ratio increases to its highest value, indicating that the amount of CO_2 injected per volume of oil produced is maximized. We can infer that saturation of the CO_2/oil interface is achieved by 0.4 PV and that the first of the two competing effects is dominant. From 0.4 PV injected to breakthrough, the crude oil that is produced contains increasing concentrations of CO_2 because it has been in contact with the injected CO_2 for sufficiently long for significant dissolution and viscosity reduction to have taken place. Consequently, the CO_2 to oil exchange ratio decreases, reaching values near zero for the end of the simple miscible CO_2 flooding process, and curtailed at its breakthrough value for the end of the primary CO_2 flooding of the CO_2-SAG process.

The produced oil was collected at regular intervals and tested for asphaltene content. It was found that the asphaltene content of the produced oil gradually decreased and dropped sharply down to 16% after the CO_2 BT. At the beginning of production, the asphaltene content in the produced oil (Figure 8b) was close to that of the stock crude oil. This initial produced oil was never in contact with the injected CO_2, but produced by displacement by oil more proximal to the CO_2 injection. Subsequently produced oil shows an increasing CO_2 concentration, resulting in increased precipitation of asphaltenes in the core, and hence decreased asphaltene content in the produced oil[2].

Before CO_2 BT, the difference in the cumulative oil RFs, GOR, R_e, and the asphaltene content in the produced oil were little during the two flooding experiments. This was because the difference in initial fluid saturation and displacement conditions in the cores of the two flooding experiments were relatively small. The difference began to appear after CO_2 BT, CO_2 was injected for secondary CO_2 flooding, and the cumulative oil recovery continued to increase effectively after the soaking process during SAG flooding. The injected CO_2 at the beginning of the secondary CO_2 flooding was mainly used to increase the fluid pressure inside the core again. At this time, the oil production rate was very slow. When the injected CO_2 amount reached 0.88 PV, the differential pressure reached the highest point for the second time. The oil production rate began to rise, but the secondary CO_2 BT occurred relatively quickly, and the oil production rate soon dropped.

Compared with simple miscible CO_2 flooding, the GOR of the CO_2-SAG secondary flooding process (Figure 7b) was relatively low at the same volume of injected CO_2. After the second CO_2 BT, the GOR of the secondary flooding increases to become higher than the GOR attained at the end of the simple miscible CO_2 flooding. In addition, the R_e value also significantly improved during the secondary CO_2 flooding (Figure 8a). This is due to the higher concentration of CO_2 in the residual oil with low viscosity and volume expansion at this stage. However, this value also dropped rapidly after the second CO_2 BT.

The asphaltene content of the oil produced during the secondary CO_2 flooding of the CO_2-SAG process (Figure 8b) remained higher than that for the simple miscible CO_2 flooding process, suggesting that less asphaltene was precipitated in the core. This is counterintuitive because it would be expected that the CO_2 soaking process would result in a large amount of asphaltenes being precipitated in the core. In the simple miscible CO_2 flooding process, this is mainly because the extraction effect of CO_2 on the light components of the crude oil being swept has a greater contribution to the oil production after the breakthrough; these small amounts of swept oil are repeatedly extracted, which only affects the structure of a small area of pores. Consequently, the components in this part of the produced oil are lighter and the asphaltenes content is also relatively low[27].

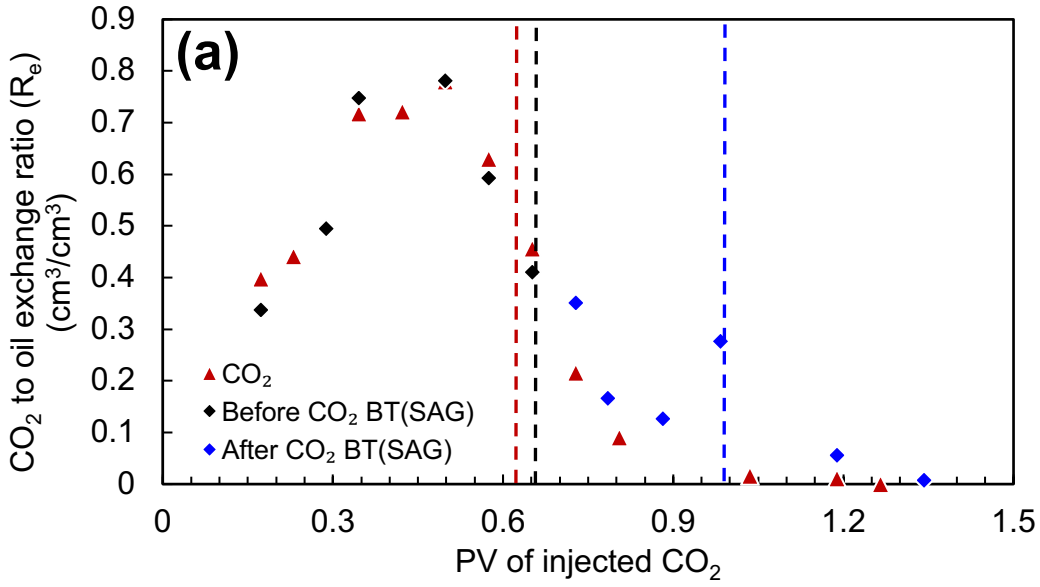

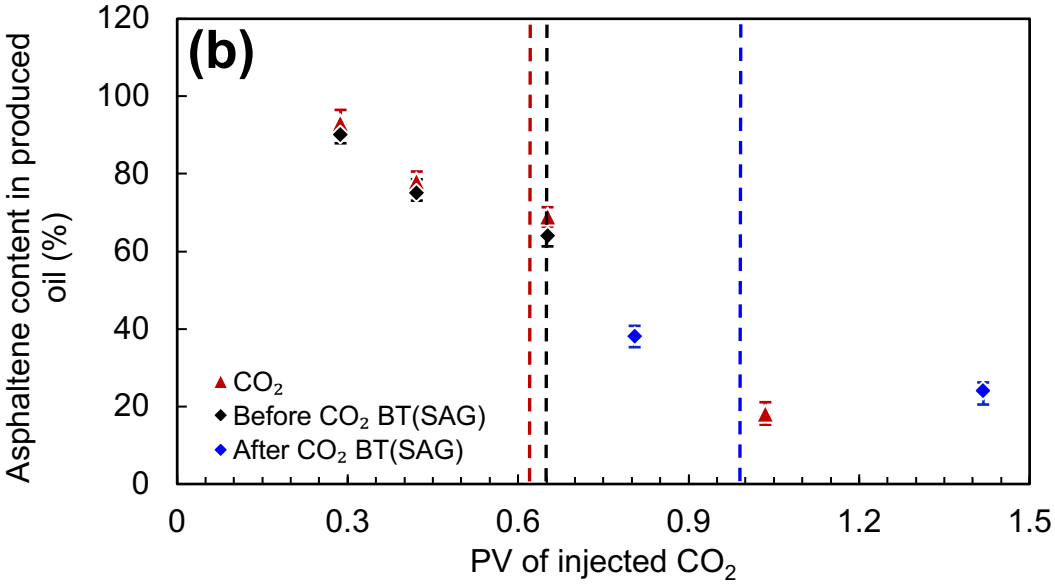

Figure 8. (a) CO_2 to oil exchange ratio, and (b) Asphaltene in produced oil both as a function of pore volumes of injected CO_2 during flooding for simple miscible CO_2 flooding (red), pre-soak (pre-breakthrough) miscible CO_2-SAG flooding (black), and post-soak secondary miscible CO_2-SAG flooding (blue). The vertical dashed lines represent the CO_2 BT for the simple miscible CO_2 flooding process (black), and the primary and secondary BTs from the CO_2-SAG process (black and blue, respectively).

Residual oil distribution

The T_2 spectra given in Figure 9 show the distribution of (i) the initial oil before flooding, and (ii) the residual oil (S_{or}) after the flooding in core plugs 2, 7 and 11 for both processes. These core plugs are located close to the inlet, in the middle, and near the outlet of the long composite core, respectively as shown schematically in the bottom part of Figure 2. In this paper these three cores were chosen as representative examples, however NMR spectra were measured for all core plugs. Since the water signal has been suppressed by our use of a Mn-rich water phase, such data can be used to calculate the recovery factor for each core. The oil RFs of all core plugs calculated from the NMR T_2 spectra are shown in Figure 10, this calculation is based on the difference of the area between the before and after curves.

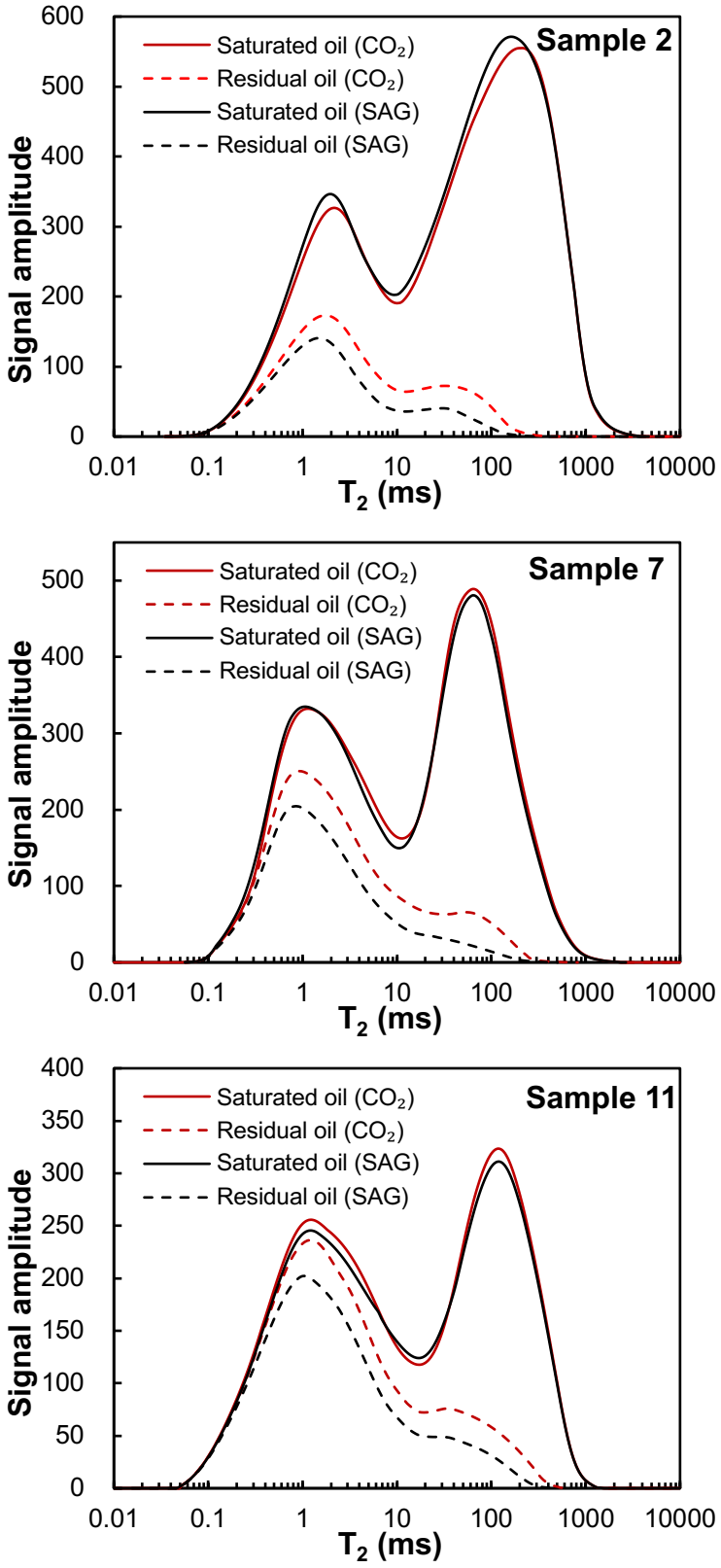

Figure 9. The initial oil distribution before flooding and residual oil after flooding by NMR T_2 spectra in core plugs 2, 7, and 11 for the simple miscible CO_2 flooding (CO_2) and the CO_2-SAG flooding process (SAG).

It is observed that the smaller the pore size, the higher the proportion of residual oil. This effect is associated with the higher capillary pressures associated with the smaller pores, which has to be overcome in order to produce the oil they contain[28]. The lower limit of the size of pores for the available oil was smaller in cores close to the injection end. This may be due to better pore-throat connectivity, longer time of CO_2-oil interaction and high mass transfer efficiency of CO_2 with the higher pressure in these cores[29]. Consequently, CO_2 can enter smaller pores to dissolve in and displace crude oil. After CO_2-SAG flooding, there was less residual oil in the cores. For cores with similar permeability, the lower limit is smaller than that after simple miscible CO_2 flooding. Because it takes a longer time for CO_2 to dissolve into the crude oil in smaller pores, the soaking process offsets this shortage, expanding and redistributing the residual oil to reach a new equilibrium in cores, weakening CO_2 breakthrough channels, and generally making the oil distribution conducive to secondary CO_2 flooding[30].

Figure 10 shows that the oil RF of each core plug decreased along the CO_2 injection direction along the long composite core. The interpretation of this figure must take into account two inter-related aspects. First, the data is likely to be affected by the core-flooding process and history. In other words, efficiency at the output end of the composite core will depend to some extent on processes that are happening or happened at the injection end. For example, the pressure at the injection end is higher than at the output, and as long as CO_2 is injected it continuously dissolves in the available crude oil along the injection direction, such that a much greater proportion of the oil near the input will be saturated with CO_2 than at the output end, a proportion of which will be produced without having CO_2 dissolved in it. Second, the core plugs were arranged to decrease in permeability along the composite core in the flow direction. Lower permeability core plugs have smaller pore-throat sizes and/or poor connectivity, resulting in poor oil displacement efficiency. Output-end core plugs are likely to naturally exhibit higher residual oil values and lower RFs. Nevertheless, the more easily produced oil from the core plugs near the injection end of the composite core must flow through these output cores in order to be produced. The steady decrease in RF for each core from the injection to the output for both the simple miscible CO_2 and the CO_2-SAG processes is expected to derive from a complex interplay of these factors, with pore size and connectivity playing an important role, but higher mass transfer efficiency of CO_2 at higher absolute

pressures and increased CO_2 dissolution towards the injection-end also playing a part.

Comparing the simple miscible CO_2 and the CO_2-SAG processes for the core plugs at the same position shows clearly that the oil RF after CO_2-SAG flooding was always greater than that attained by simple miscible CO_2 flooding. We have also calculated the percentage improvement in RF by using CO_2-SAG flooding instead of simple miscible CO_2 flooding using the equation $\Delta\mathrm{RF}(\%) = RF_{CO_2-SAG} - RF_{Simple\ CO_2}$, which is also shown in Figure 10. When quantified this way, the improvement in RF is about 7% at the injection end of the core, and gradually increases to about 12% at the output (low permeability) end of the composite core. This is an important result, because it shows that while CO_2-SAG flooding is significantly better than simple miscible CO_2 flooding over a wide range of permeabilities, it is particularly effective for lower permeability rocks which might otherwise retain a significant unproduced hydrocarbon volume.

It is perhaps unsurprising that the soaking process is more beneficial to the RF of rocks with low permeability and high residual oil saturation. Not only do the low permeability cores present more potential for augmented oil production because they would otherwise retain a greater residual oil volume, the soaking process is designed particularly to allow time for the CO_2 to have more access to the oil in these more difficult to reach pores.

Figure 11 shows ΔRF as a function of different pore size ranges measured using NMR data for core plugs 2, 7, and 11. The oil recovery from different sizes of pores in cores with different permeability and different positions was improved to different degrees by implementing the soaking process, but never degraded. The pores with T_2 in the range 1-100 ms (medium size) of the three cores show the relatively larger increase in oil production, the smallest (0.1-1 ms) and largest (100-1000 ms) had relatively little improvement. There is little scope for RF improvement in the large pores because these pores are already effectively purged of oil by a simple miscible CO_2 flood. Nevertheless, the soaking manages a significant improvement of 5.2% to 10.2% dependent on core plug position. The best improvement is in the low permeability rocks at the output end, which we can attribute to a compensation for the low connectivities of these low permeability rocks previously generating a few

BT channels with consequent by-passing of oil not connected by a channel even if the pores are individually large.

There is also a small improvement for the very smallest pores (5.6% to 7.8%). The improvement for these small pores is limited because these pores are so small that the soaking process is insufficient to allow their oil to become completely saturated with CO_2. A longer soaking time would allow better access to these pores, but at the expense of saturating the water in the medium and large sized pores (the dissolution of CO_2 can make irreducible brine become movable brine), which would nullify any gain in RF. The improvement in RF from the smallest pores was better in the lower permeability output-end cores, which is probably because these rocks have a greater proportion of small pores, and hence there is greater scope for RF improvement.

The greatest benefit was found to be in the medium pore size ranges (1-100 ms). It is these pores that share a number of characteristics. First, they are large enough to provide a significant increase in RF if their oil is able to be produced. Second, they are small enough to be by-passed by the BT channels which result from the initial CO_2 flooding as these channels will preferably follow the well-connected larger pore sizes. Third, being by-passed the oil they contain has little contact with the CO_2 from the initial flooding. Fourth, the medium-sized pores are fairly easily accessible for the CO_2 from the soaking process in a reasonably short soaking time. Fifth, the reasonable connectivity experienced by medium-sized pores would allow the swelled, lower viscosity oil they contain to be swept into existing and new BT channels by the secondary flood.

We note that the greatest improvement was always for core plug 11, irrespective of pore size due to the sufficient residual oil in all pores of core plug 11 at the outlet end after CO_2 BT. This observation is important for the production of heterogeneous reservoirs, where CO_2-SAG flooding has a clear advantage of other EOR options.

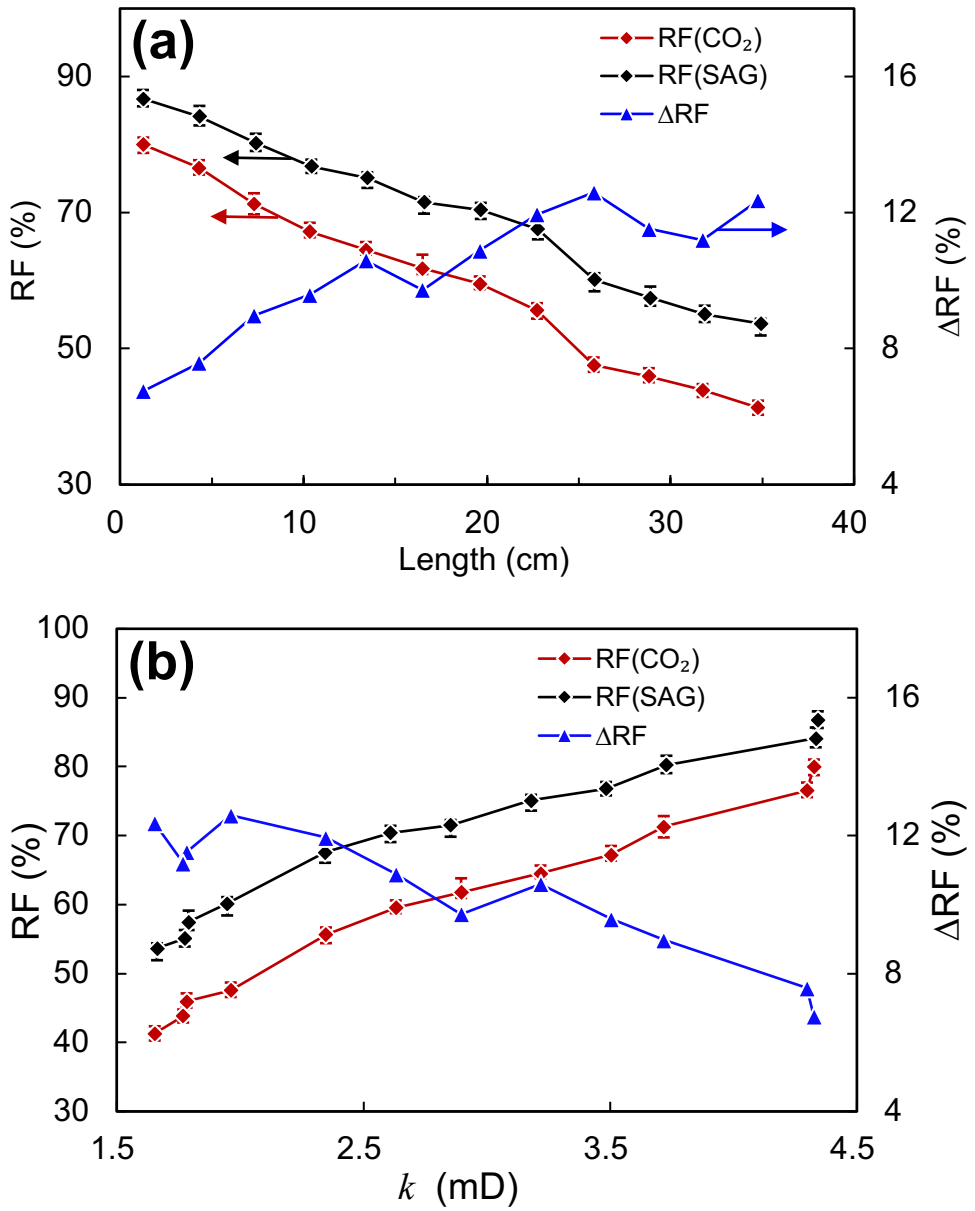

Figure 10. The oil RF of each core plug along the long composite cores after flooding as a function of (a) position, and (b) initial core plug permeability using simple miscible CO_2 flooding (red) and CO_2-SAG flooding (black), together with the difference in the oil RF between the two flooding processes $\Delta RF(\%) = RF_{CO_2-SAG} - RF_{Simple\ CO_2}$.

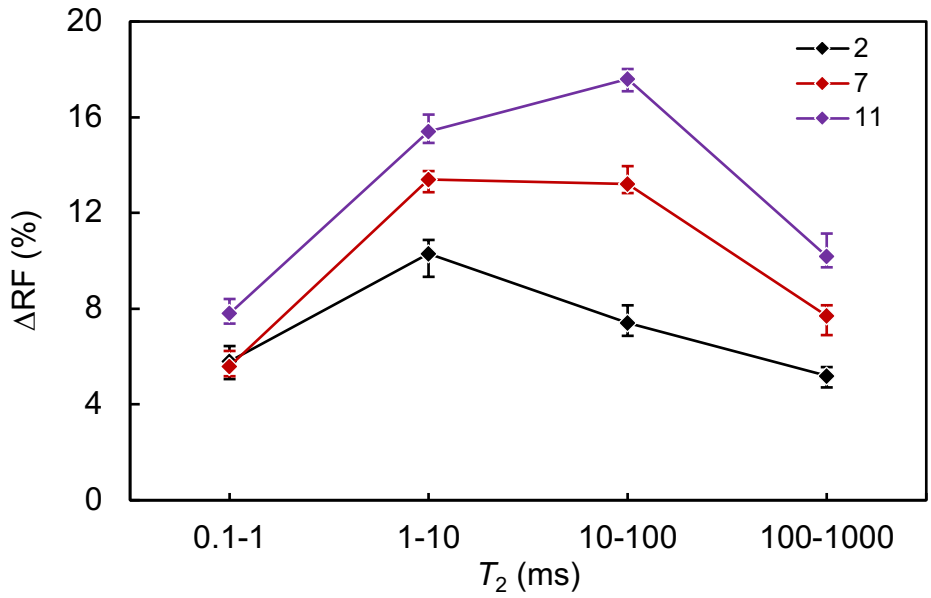

Figure 11. The value of ΔRF as a function of different pore size ranges measured using NMR data for core plugs 2, 7, and 11.

Permeability damage

We have quantified permeability damage using a permeability decline parameter, k_d, where k_d=100×(k_{before}−k_{after})/k_{before}. Figure 12 shows this parameter for both flooding processes. We have also calculated the percentage difference in k_d between using CO_2-SAG flooding and simple miscible CO_2 flooding using the equation $\Delta k_d(\%) = k_{d\_CO2-SAG} - k_{d\_Simple\ CO2}$, which is also shown in Figure 12.

Similar values and a similar pattern of permeability decline results from both flooding processes. Both processes induce an 8.8% to 27.9% decline in permeability dependent on location within the composite core. The core plugs near to the injection end of the composite core undergo a permeability decline of approximately 20% (19.1% to 20.1%, depending on flooding process), which becomes greater as one moves along the composite core in the direction of flow (and therefore to core plugs of progressively increasing initial permeability). This increase in permeability decline occurs until core plug 4, which presents the largest permeability decline at approximately 27% (26.7% to 27.9%, depending on flooding process). From core plug 5 onwards, there is progressively less permeability damage, as the initial permeability decreases further, until the lowest permeability core plugs at the output end of the composite core undergo a permeability decline of between 8.8% and 12.4%, depending on the flooding

process. This pattern of permeability decline is the same for both core-flooding processes, but the CO_2-SAG process produces a slightly larger declines. The difference between the permeability declines is shown by the blue curve in Figure 12, which is erratic. Calculation of the mean value and standard deviations of these data show that the CO_2-SAG process produces a larger permeability decline than the simple miscible CO_2 process by an average of 2.49±1.19%. There is no evidence for a physical reason underlying the apparent erratic or oscillating nature of Δk_d, which is most likely a statistical artefact, although the slightly larger difference towards the output end may be a real effect. It may also be that not only the core permeability is different, but the pore-throat structure and pore size distribution are also different. These have different sensitivities to the permeability damage caused by asphaltene precipitation. It may also be that the connection between cores with different permeability is not as smooth as the connection of a whole long block of heterogeneous cores.

That the CO_2-SAG process induces slightly more damage is consistent with the view that the greater volumes of CO_2 which dissolve in the residual oil during the soaking process should result in the precipitation of more asphaltene, which has the potential for narrowing and blocking pore throats[31]. The combination of an observed decline in core permeability (Figure 12) with a reduction in concentration of asphaltene in the produced oil compared to that in the initial oil (Figure 8b) suggests strongly that asphaltene precipitation is occurring. Small asphaltene particles precipitate from crude oil, gradually enlarging and aggregating as the oil carries them through the core. The particles become trapped when they become as large or larger than the size of the pore-throats. The trapped asphaltene blocks the pore-throat, reducing the hydraulic connectivity of the rock, and hence reducing the permeability of the reservoir. Concurrently, asphaltene precipitates are adsorbing onto the surfaces of the rock matrix, gradually reducing the size of both pores and pore-throats, which predisposes asphaltene precipitates to block the pore-throats[32]. These adsorbed asphaltenes also change the wettability of the matrix, making it more oil-wet[33]. However, it is worth noting that while asphaltene precipitation can reduce the permeability of a rock substantially, it has little effect on porosity[5,34].

We hypothesize that the degree of permeability decline is determined by the scale of asphaltene precipitation and particle migration in pore-throat, the initial permeability and the connectivity of the

pore throat structure of cores. Furthermore, we recognize that higher oil RF (of both the core plugs in the experiment and rocks in the reservoir) is an indicator that more crude oil has interacted with the injected CO_2, that there has been a larger swept volume of injected CO_2, and hence there will have been more asphaltene precipitation. The greater degree of asphaltene precipitation thus provides a greater number of particles to migrate towards pore-throats, and hence there is a greater the chance of pore-throat blockage, and a greater decline in permeability[13].

The profile of the permeability decline was noted to be smoother for the CO_2-SAG flooding process than for the simple miscible process, which may result from the soaking process producing a more uniform deposition of asphaltene, but further comparative core-flooding experiments would have to be carried out to confirm this.

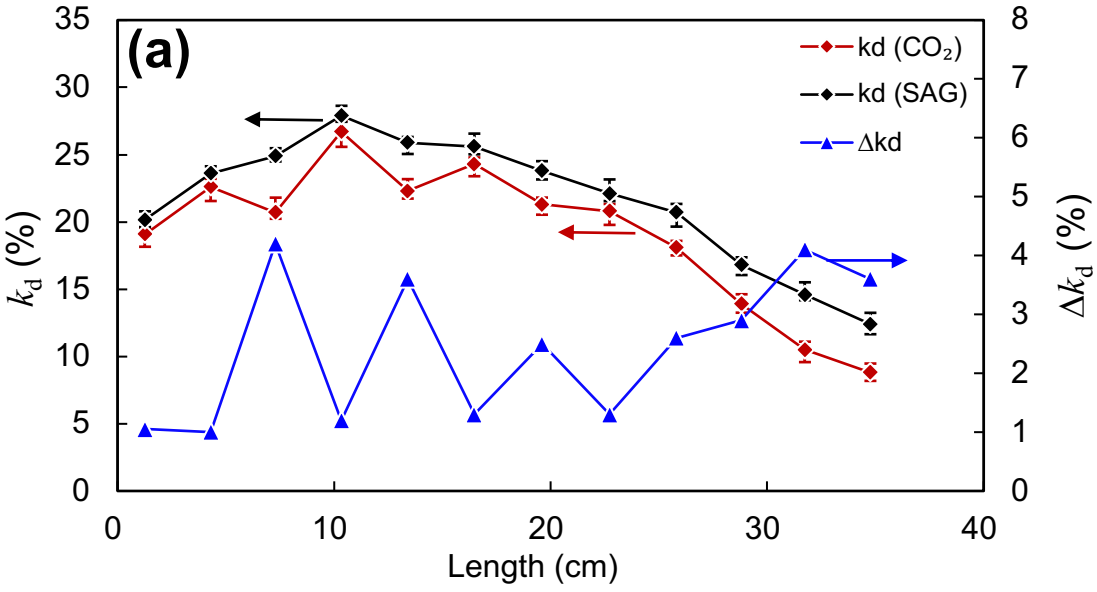

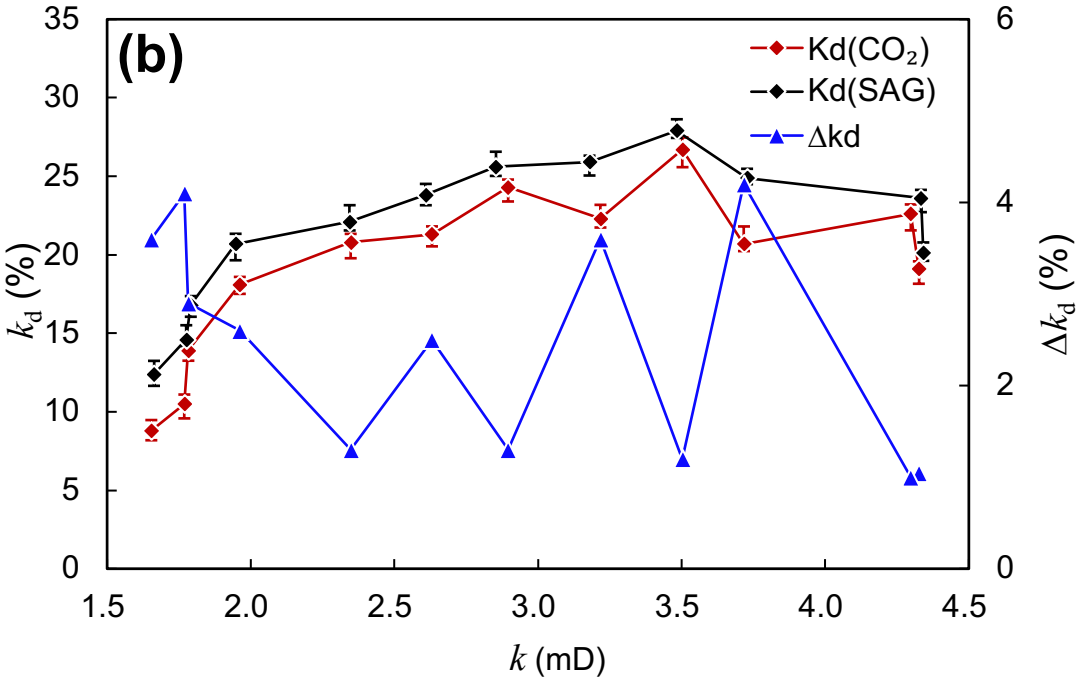

Figure 12. The permeability decline of each core plug along the composite core as a function of (a) position, and (b) initial core plug permeability after simple miscible CO_2 flooding (red) and after CO_2-SAG flooding (black), together with the percentage change in permeability decline with respect to the simple miscible CO_2 flooding process (blue).

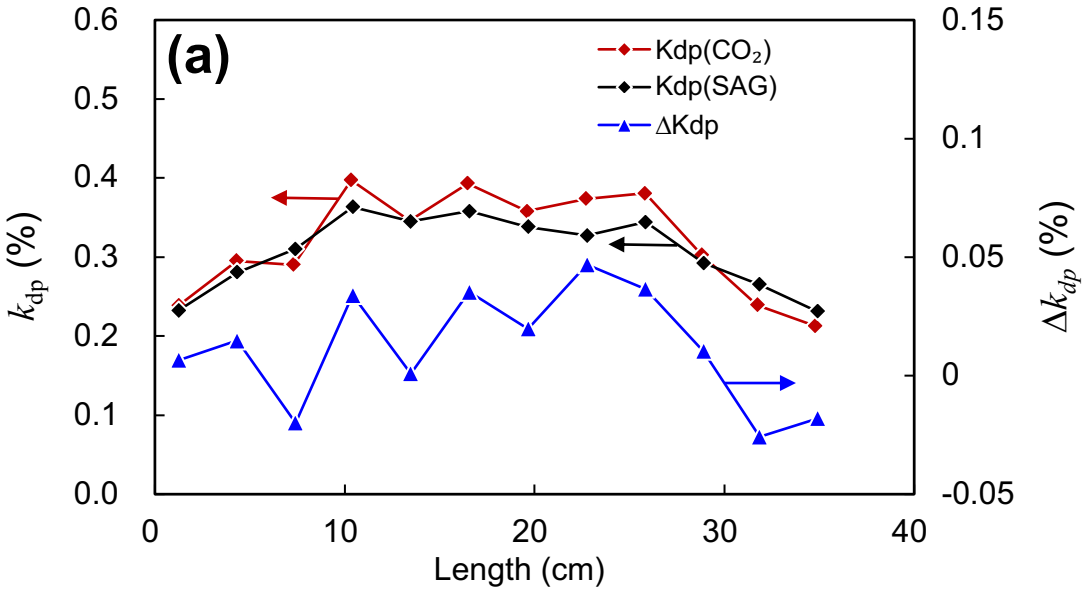

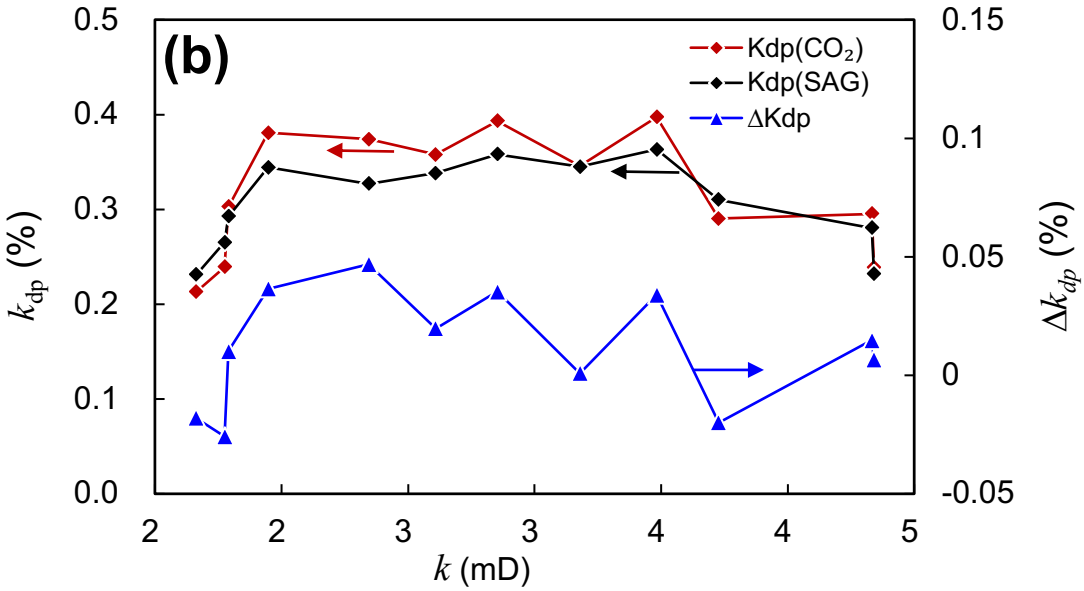

Figure 13. The k_{dp} and Δk_{dp} values of each core plug along the long composite core after flooding as a function of (a) position, and (b) initial core plug permeability.

The CO_2-SAG flooding causes a greater decrease in permeability and a higher oil RF than the CO_2 flooding. We have defined a value of k_{dp} to combine the improvement of oil recovery and permeability damage in a single parameter, where $k_{dp} = k_d$/RF. The parameter k_{dp} represents the permeability decrease (damage) per unit increase in oil RF, where small values are better than large values as they represent smaller degrees of permeability damage per increase in produced oil.

Figure 13 shows the k_{dp} parameter for both flooding processes. We have also calculated the percentage difference in k_{dp} between using CO_2-SAG flooding and simple miscible CO_2 flooding using the equation $\Delta k_{dp}(\%) = k_{dp\_CO2-SAG} - k_{dp\_Simple\ CO2}$, which is also shown in Figure 13. The curves for the two flooding processes are remarkably similar both in value and pattern. Small values of about 0.23% occur at the input and output ends of the composite core, while values rise to approximate 0.36% to 0.30% in the middle of the composite core. A statistical comparison of the two curves shows that they are not statistically distinguishable at a probability of 5%, although qualitatively, it seems that the CO_2-SAG flooding process may be marginally better towards the middle of the composite core.

The final stages of the experimental protocol involved complete cleaning of the cores of all fluids and

asphaltene. When this was carried out, it was noted that the permeability of cores did not fully recover to their initial values. We define k_{di} to be the unrecovered permeability decline, i.e., the permeability decline that is not recovered by full cleaning of the core from all traces of asphaltene. Similarly to our previous definition of k_d, k_{di} is expressed as a percentage with respect to the initial permeability, which allows it to be compared directly with k_d. Furthermore, we also define the parameter R_{kd} to be the percentage of k_{di} in the total permeability decline, which is given by $R_{kd}=k_{di}/k_d\times100$.

The k_{di} and R_{kd} values of core plugs after both simple miscible CO_2 flooding and CO_2-SAG flooding are given in Figure 14, together with the difference in the k_{di} values between the two flooding processes Δk_{di}. The values of k_{di} and R_{kd} for the simple miscible CO_2 flooding varied between 0.4-1.9% and 8.8%-3.9%, respectively, and for the CO_2-SAG flooding process varied in the ranges 0.6-2.9% and 12.1%-4.1%, again respectively, while the value of Δk_{di} varied between 0.2%-4%. For both processes there was a general trend that there was greater unrecoverable permeability damage in the first 60% of the composite core and that the proportion of overall damage that could be attributed to unrecoverable permeability damage decreased along the composite core in the flow direction. This implies that unrecoverable damage was correlated to initial permeability, with larger initial permeabilities being associated with larger values of both unrecoverable permeability damage and the proportion of overall damage that could be attributed to unrecoverable permeability damage. We have already seen that the CO_2-SAG process results in greater overall permeability damage (Figure 12). It is clear from Figure 14 that the CO_2-SAG process also results in greater unrecoverable permeability damage which also represents a greater proportion of the overall permeability damage.

We attribute the unrecoverable permeability damage to CO_2–brine–rock interactions, but it has relatively less effect on permeability variation than asphaltene precipitation, in our work making up only 3.9-12.1% of the overall permeability damage[35]. This insignificant effect has been attributed to (i) the limited contact area between CO_2, brine and rock, and (ii) the core-flooding time not being conducive to CO_2–brine–rock interactions.

The values of k_{di} and R_{kd} were higher after CO_2-SAG flooding because the soak ensures that this process

has a longer CO_2–brine–rock interaction time. Cores with larger permeabilities at the injection end of the composite core also experienced greater unrecoverable permeability decline also because there is greater time available for CO_2–brine–rock interactions to occur, but also over a larger pore volume. The soaking process exacerbated this difference, that is, ΔR_{kd} is larger the closer the core plug is to the injection face of the composite core. The R_{kd} value after these long composite core flooding experiments is higher than the short core CO_2 flooding experiment carried out by Wang et al., where R_{kd}<5%[9]. This may be attributed to the higher content of carbonate minerals and clay minerals in the core used in this experiment as well as the longer displacement time.

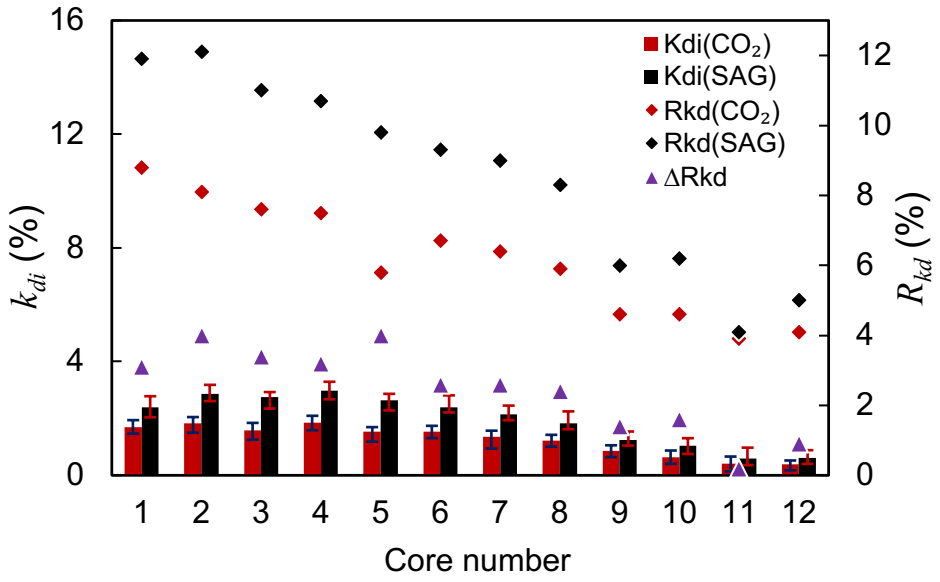

Figure 14. The values of k_{di}, R_{kd} and ΔR_{kd} of each core plug.

Variation in Brine Saturation

The T_2 spectra given in Figure 15 show the brine distributions before flooding and when re-saturated with brine after flooding for core plugs 2, 7 and 11. The core was cleaned and aged in brine while asphaltene precipitation remained trapped in the pores before being resaturated. The variation in brine saturation $S_{wv} = S_{wb}–S_{wa}$ was calculated, where S_{wb} is the brine saturation before flooding (the solid line in Figure 15), and S_{wa} is the brine re-saturation after flooding (the dashed line in Figure 15). Hence, S_{wv} represents the change in the brine saturation of the cores due to the flooding. Brine re-saturation after flooding is affected by two mechanisms. The first is the blockage of the pore-throats, and the second is wettability alteration[36]. In the first case, the migration of asphaltene particles blocks pore throats so

that pores cannot be fully re-saturated with brine []. This results in the signal amplitude of that part of the T_2 spectrum representing small pores or pores connected by small pore throats (T_2<10 ms) showing a significant decline in amplitude after re-saturation. In the second case, the asphaltene adsorbs to pore surfaces, making them more oil-wet. This results in a decrease in the amplitude of that portion of the T_2 spectrum representing larger pores (T_2>10 ms), because gas and oil have promoted asphaltene precipitation only in these larger pores. Both of these factors play a role in resisting water re-saturation, as can be observed in Figure 15, where reductions in the amplitude of the T_2 spectrum exist at both large and small values of T_2, and consequently there is an increase in the value of S_{wv}.

The value of S_{wv} represents the comprehensive influence of blockage caused by asphaltene precipitation and the variation of wettability caused by adsorption of asphaltene precipitation in the pores on the petrophysical properties of the cores. As shown by the results of miscible CO_2 flooding experiments on similar cores[5], the changes in wettability caused by the adsorption of asphaltene precipitation have a greater impact on the value of S_{wv}. The large pores and associated pore throats are the main conduits for CO_2 flooding and hence asphaltene precipitation. Consequently the signal amplitude of large pores measured by the T_2 spectrum is reduced. The signal amplitude of resaturated brine decreases more after SAG flooding.

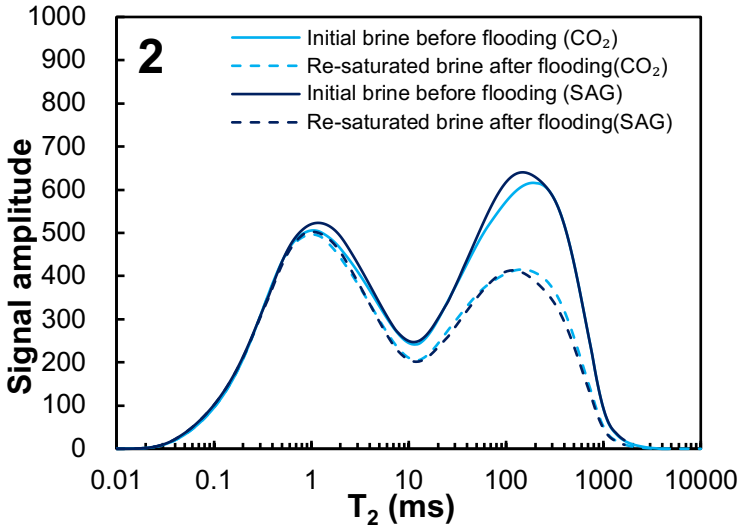

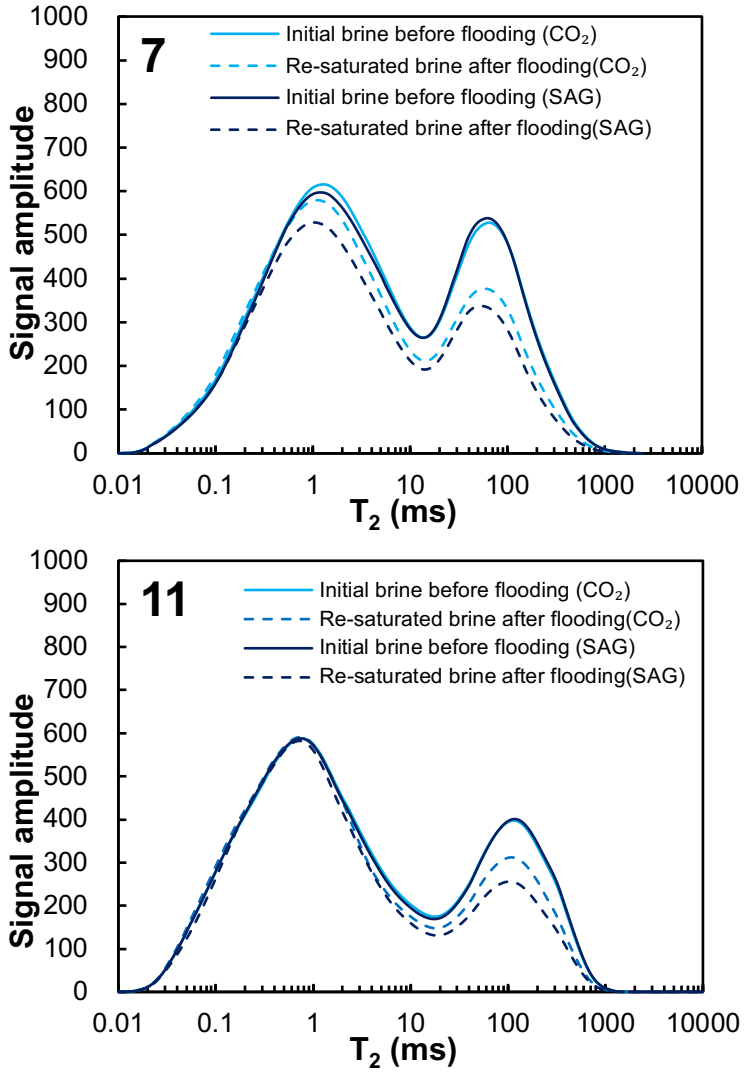

Figure 15. NMR T_2 spectra of brine distribution in cores showing initial brine before flooding and the restored saturations after flooding and cleaning for cores 2, 7 and 11.

The values of S_{wv} for each of the flooding processes and for each of the core plugs composing the composite core are given in Figure 16, together with the values of the difference in S_{wv} between the two flooding processes, given by $\Delta S_{wv} = S_{wv\_CO2\text{-}SAG} - S_{wv\_CO2}$. For the simple miscible CO_2 flooding the value of S_{wv} gradually decreases along the flow direction, which is consistent with the distribution of residual oil saturation. The high saturation of residual oil means that the swept volume of CO_2 is smaller and the interaction of CO_2 and oil is low. The scale of asphaltene precipitation and the range of pores involved was small, and the variation of core wettability was also small, resulting in small S_{wv} values. The soaking process caused more asphaltene precipitation in more pores, the S_{wv} value was greater after CO_2-SAG

flooding, and the distribution increased and then fell, with the largest S_{wv} in the middle of the long composite core. Furthermore, the difference in S_{wv} after CO_2-SAG flooding and simple miscible CO_2 flooding increased along the flow direction.

Figure 17 shows how the value of ΔS_{wv} varies with pore size classes for core plugs 2, 7 and 11. In core plug 2, ΔS_{wv} is small and distributed uniformly over all pore sizes. This is because oil in the cores near the injection face with large permeabilities is already efficiently produced by the simple miscible CO_2 flooding process. The increase in ΔS_{wv} in pores of all size in core plugs 7 and 11 was greater than that of core plug 2, and the larger the pore size, the greater increase in ΔS_{wv}, but the increase in the large pores with T_2 at 100-1000ms was not the largest. This indicated that the promotion of asphaltenes precipitation and adsorption by the soaking process in the pores with T_2 at 1-100ms was greater in cores located in the middle and near the outlet of the composite core, and hence had a greater impact on wettability changes.

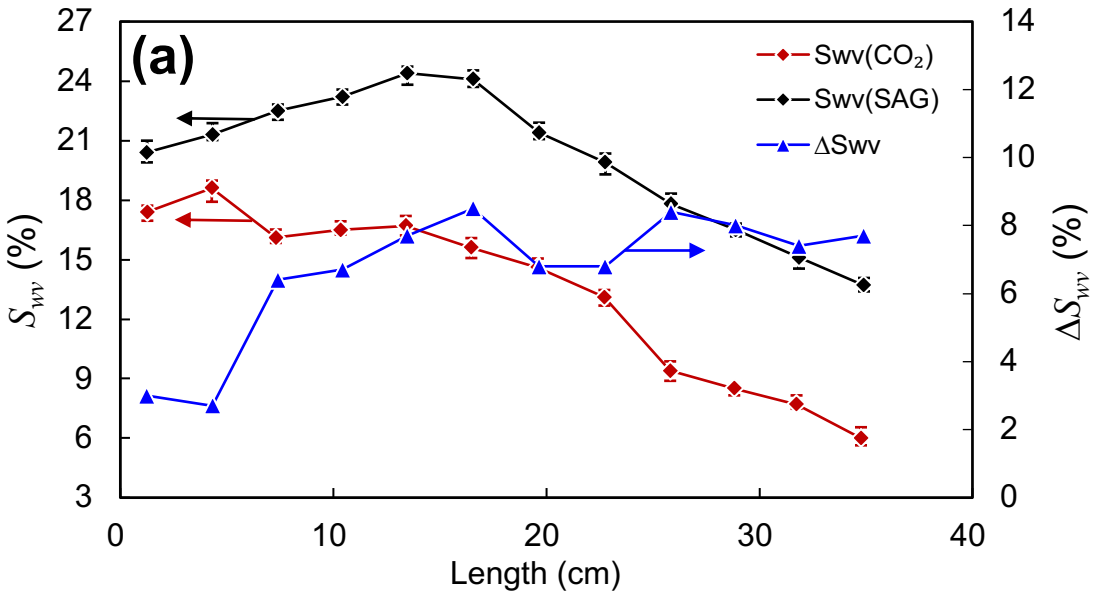

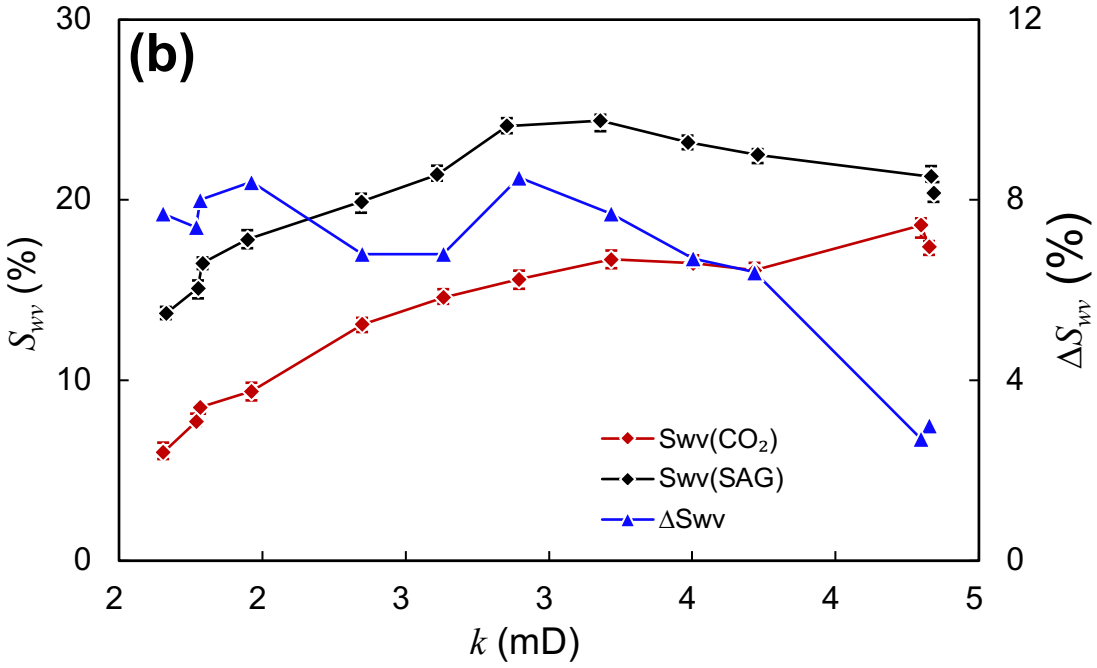

Figure 16. The S_{wv} value of each core plug along the long composite cores after flooding as a function of (a) position, and (b) core plug initial permeability.

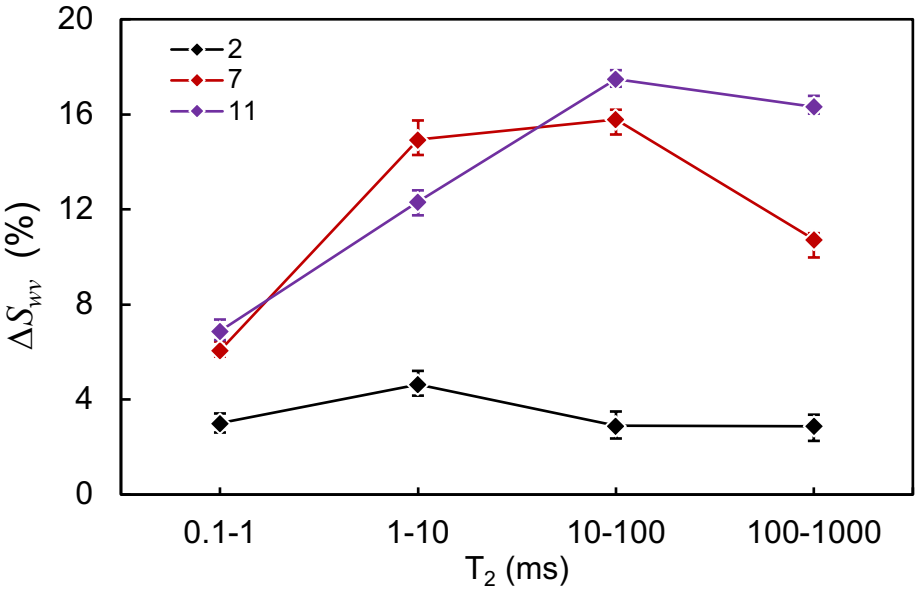

Figure 17. Increase in S_{wv} after CO_2-SAG flooding in different size of pores compared with the S_{wv} after simple miscible CO_2 flooding in core plugs 2, 7, 11.

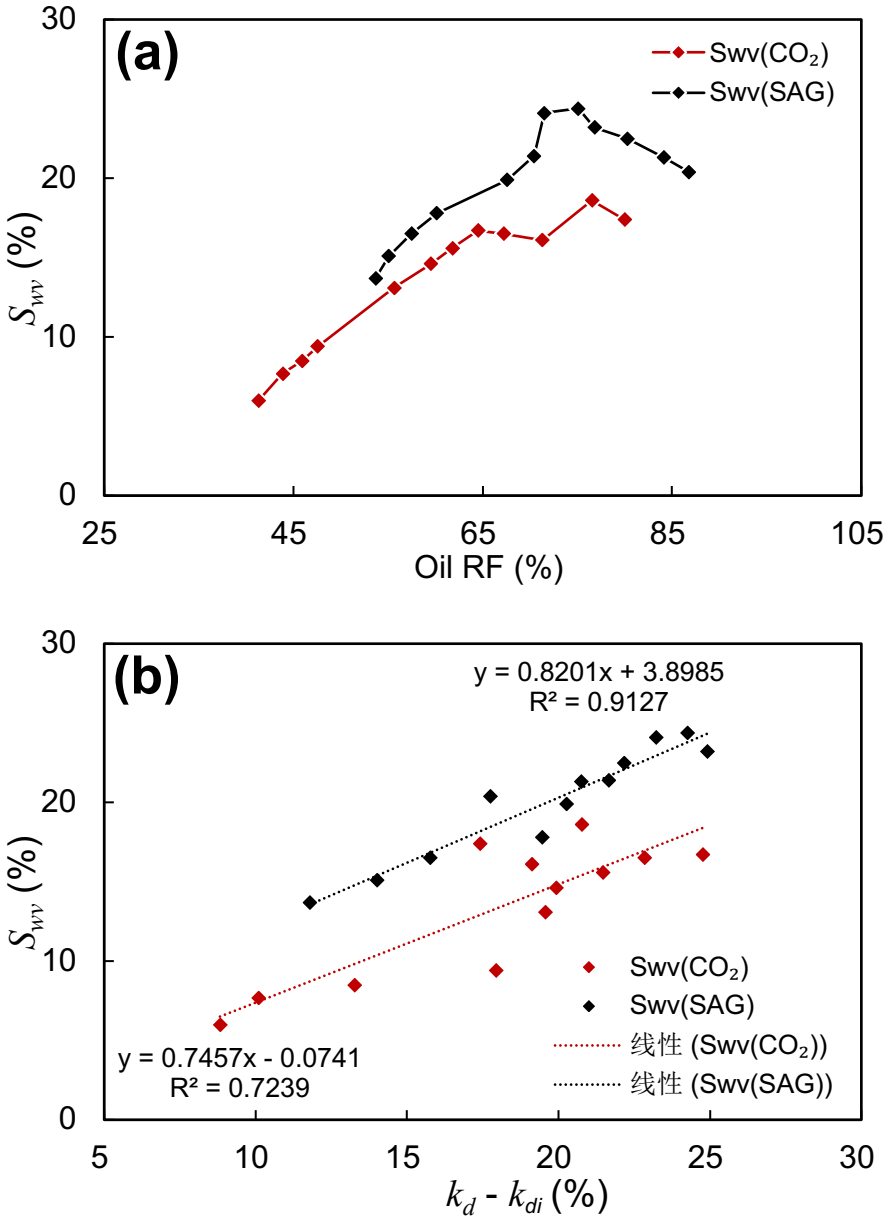

Figure 18. (a) The S_{wv} as a function of oil RF for each core plug after CO_2-SAG and simple miscible CO_2 flooding. (b) The S_{wv} as a function of k_d -k_{di} after CO_2-SAG and simple miscible CO_2 flooding.

The relationship between S_{wv} and oil recovery for each of the two flooding processes is shown in Figure 18a. Considering Figure 18a, it is clear that those parts of the core which have larger recovery factors generally have larger values of S_{wv} because the resaturated water occupies the space vacated by the produced oil. In principle the curves for the two processes should be collinear. That the CO_2-SAG curve covers an overlapping but higher range of RF values is simply an indicator that this process can potential lead to better recoveries. That the CO_2-SAG curve covers an overlapping but slightly higher range of

S_{wv} values is not expected as residual wettability changes, which might be expected to be greater for the CO_2-SAG process would produce lower rather than higher values of S_{wv} (i.e., separation of the curves by a vertical relative movement). We hypothesize that although the oil in some small pores interacted with CO_2 during the soaking phase of the CO_2-SAG process, this oil was not effectively driven out in the secondary flooding process with less asphaltene particle migration and less pore blockage. Consequently, there is less improvement of oil recovery than might be attained if the secondary flood were more efficient. Nevertheless, the soaking phase of the CO_2-SAG process still caused asphaltene precipitation, and asphaltene adsorption still resulted in changes in wettability (i.e., separation of the curves by a horizontal relative movement).

The relationship between S_{wv} and permeability decline for each of the two flooding processes is shown in Figure 18b. Both curves are linear and parallel. At least, when fitted by a linear equation their gradients (0.6995 and 0.6985 for CO_2-SAG and simple CO_2 flooding, respectively) are effectively identical. Once again the CO_2-SAG process exhibits apparently higher resaturation values. Although difficult to interpret, these observations may indicate that the improvement of the secondary flood might produce even better EURs.

Conclusions

The process of the reservoir condition miscible CO_2-SAG process was studied for a low permeability long composite core composed of 12 core plugs with decreasing permeability along the flow direction, and quantifying the distribution of differential pressure, oil recovery factor, residual oil asphaltene precipitation permeability damage and wettability variation comparing with simple CO_2 flooding.

- The effective differential pressure for oil displacement was maintained for a shorter time during secondary flooding of CO_2-SAG flooding. The differential pressure consumed by the 8 cm long lower permeability cores at the outlet accounted for 40-70% of the total differential pressure.
- The overall oil recovery factor was 72.8% after CO_2-SAG flooding, 11% higher than CO_2 flooding. The oil recovery factors of core plugs after CO_2-SAG flooding vary between 53% and 87%, compared with 41-80% after simple miscible CO_2 flooding. The values decreased along the CO_2

flow direction. However, the improvement in oil production by the soaking process gradually increases along the CO_2 flow direction compared with CO_2 flooding in all core plugs. This is attributable to the soaking process mitigating the insufficient interaction between crude oil and CO_2 in cores with low permeability and high residual oil saturation close to the outlet before CO_2 BT.

- The permeability decline experienced by core plugs that is caused by asphaltene precipitation after CO2-SAG flooding was 8-20%, 1-4.5% higher than that for simple miscible CO_2 flooding. The overall decline in core permeability at the injection end is greater than at the outlet end. The difference in permeability decline was slightly larger towards the output end after two flooding experiments. Permeability damage can also be caused by CO_2–brine–rock interactions, 4-12% of the total permeability decline after SAG flooding, larger than that of simple miscible CO_2 flooding.
- The variation of core wettability due to asphaltene precipitation gradually decreased along the injection direction after CO_2 flooding, which is consistent with the distribution of residual oil saturation. The variation was larger after SAG flooding, and reached the largest in the middle of the long composite core; the soaking process promotes the precipitation and adsorption of asphaltenes. The impact of the soaking process on the transformation of rock wettability to oil-wet was greater than that of permeability decline.

The results show the advantages of CO_2-SAG flooding in the improvement of oil production in heterogeneous reservoirs with higher injected CO_2 utilization efficiency, although the asphaltene precipitation blockage is more serious, and the degree of wettability variation is greater. When the reservoir is assessed to have strong heterogeneity, CO_2-SAG flooding is a more advantageous measure that should be selected. If measures can be taken to inhibit the precipitation of asphaltenes in the reservoir (for example, the injection of inhibitors), CO_2-SAG flooding is expected to achieve better oil production improvement.

Acknowledgments

Thanks are given to the China Scholarship Council for funding the opportunity of the lead author to research at The University of Leeds, UK. This research is supported by National Natural Science Foundation of China, “Study on the physical basis of seepage in extra-deep clastic reservoirs” (51774300).

References

(1) Wang, X. and Gu, Y., 2011. Oil recovery and permeability reduction of a tight sandstone reservoir in immiscible and miscible CO_2 flooding processes. *Industrial & Engineering Chemistry Research*, *50*(4), pp.2388-2399.

(2) Cao, M. and Gu, Y., 2013. Oil recovery mechanisms and asphaltene precipitation phenomenon in immiscible and miscible CO_2 flooding processes. *Fuel*, *109*, pp.157-166.

(3) Wang, L., He, Y., Wang, Q., Liu, M. and Jin, X., 2020. Multiphase flow characteristics and EOR mechanism of immiscible CO_2 water-alternating-gas injection after continuous CO_2 injection: A micro-scale visual investigation. *Fuel*, *282*, p.118689.

(4) Shen, Z. and Sheng, J.J., 2018. Experimental and numerical study of permeability reduction caused by asphaltene precipitation and deposition during CO_2 huff and puff injection in Eagle Ford shale. *Fuel*, *211*, pp.432-445.

(5) Wang, Q., Yang, S., Glover, P.W., Lorinczi, P., Qian, K. and Wang, L., 2020. Effect of Pore-Throat Microstructures on Formation Damage during Miscible CO_2 Flooding of Tight Sandstone Reservoirs. *Energy & Fuels*, 34(4), 4338-4352.

(6) Jafari Behbahani, T., Ghotbi, C., Taghikhani, V. and Shahrabadi, A., 2012. Investigation on asphaltene deposition mechanisms during CO_2 flooding processes in porous media: a novel experimental study and a modified model based on multilayer theory for asphaltene adsorption. *Energy & fuels*, *26*(8), pp.5080-5091.

(7) Glover, P.W., Lorinczi, P., Al-Zainaldin, S., Al-Ramadhan, H., Sinan, S. and Daniel, G., 2019, September. A Fractal Approach to the Modelling and Simulation of Heterogeneous and Anisotropic Reservoirs. In *SPE Offshore Europe Conference and Exhibition*. Society of Petroleum Engineers.

(8) Wang, Z., Yang, S., Lei, H., Yang, M., Li, L. and Yang, S., 2017. Oil recovery performance and permeability reduction mechanisms in miscible CO_2 water-alternative-gas (WAG) injection after continuous CO_2 injection: An experimental investigation and modeling approach. *Journal of Petroleum Science and Engineering*, *150*, pp.376-385.

(9)Wang, Q., Yang, S., Lorinczi, P., Glover, P.W. and Lei, H., 2019. Experimental Investigation of Oil Recovery Performance and Permeability Damage in Multilayer Reservoirs after CO_2 and Water–Alternating-CO_2 (CO_2–WAG) Flooding at Miscible Pressures. *Energy & Fuels*, 34(1), 624-636.

(10) Li, Z. and Gu, Y., 2014. Soaking effect on miscible CO_2 flooding in a tight sandstone formation. *Fuel*, *134*, pp.659-668.

(11) Norouzi, H., Rostami, B., Khosravi, M., & Shokri Afra, M. J.,2019. Analysis of secondary and tertiary high-pressure gas injection at different miscibility conditions: mechanistic study. *SPE reservoir evaluation & engineering*, *22*(01), 150-160.

(12) Li, Z., 2014. *Optimum Timing for CO_2-EOR After Waterflooding and Soaking Effect on Miscible CO_2 Flooding in a Tight Sandstone Formation* (Doctoral dissertation, Faculty of Graduate Studies and Research, University of Regina).

(13) Wang, Q., Wang, L., Glover, P. and Lorinczi, P., 2020. Effect of pore-throat microstructure on miscible CO_2 soaking-alternating-gas (CO_2-SAG) flooding of tight sandstone reservoirs. *Energy & Fuels*.

(14) Zhang, J., Zhang, H.X., Ma, L.Y., Liu, Y. and Zhang, L., 2020. Performance evaluation and mechanism with different CO_2 flooding modes in tight oil reservoir with fractures. *Journal of Petroleum Science and Engineering*, *188*, p.106950.

(15) Al-Mudhafar, W.J., Rao, D.N. and Srinivasan, S., 2018. Reservoir sensitivity analysis for heterogeneity and anisotropy effects quantification through the cyclic CO_2-Assisted Gravity Drainage EOR process–A case study from South Rumaila oil field. *Fuel*, *221*, pp.455-468.

(16) Lei, H., Yang, S., Qian, K., Chen, Y., Li, Y. and Ma, Q., 2015. Experimental investigation and application of the asphaltene precipitation envelope. *Energy & Fuels*, *29*(11), pp. 6920-6927.

(17) Kord, S., Mohammadzadeh, O., Miri, R. and Soulgani, B.S., 2014. Further investigation into the mechanisms of asphaltene deposition and permeability impairment in porous media using a modified analytical model. *Fuel*, *117*, pp. 259-268.

(18) Lei, H., Yang, S., Zu, L., Wang, Z. and Li, Y., 2016. Oil recovery performance and CO_2 storage potential of CO_2 water-alternating-gas injection after continuous CO_2 injection in a multilayer formation. *Energy & fuels*, *30*(11), pp.8922-8931.

(19) Duan, X., Hou, J., Zhao, F., Ma, Y. and Zhang, Z., 2016. Determination and controlling of gas channel in CO_2 immiscible flooding. *Journal of the Energy Institute*, *89*(1), pp.12-20.

(20)Mi Mosavat, N., & Torabi, F.,2016. Micro-optical analysis of carbonated water injection in irregular and heterogeneous pore geometry. *Fuel*, *175*, 191-201.

(21) Li, Z. and Dong, M., 2009. Experimental study of carbon dioxide diffusion in oil-saturated porous media under reservoir conditions. *Industrial & engineering chemistry research*, *48*(20), pp.9307-9317.

(22) Li, S., Qiao, C., Li, Z. and Hui, Y., 2018. The effect of permeability on supercritical CO_2 diffusion coefficient and determination of diffusive tortuosity of porous media under reservoir conditions. *Journal of CO_2 Utilization*, *28*, pp.1-14.

(23) Ssebadduka, R., Kono, H., Sasaki, K., Sugai, Y. and Nguele, R., 2020. Measurements of CO_2 molecular diffusion coefficients in crude oils from swelling-time curve and estimation using viscosity from the Stokes-Einstein formula. Journal of Petroleum Science and Engineering, 187.

(24) Yang, D., Gu, Y. and Tontiwachwuthikul, P., 2008. Wettability determination of the reservoir brine-reservoir rock system with dissolution of CO_2 at high pressures and elevated temperatures. *Energy & Fuels*, *22*(1), pp.504-509.

(25) Cao, M., & Gu, Y.,2013. Physicochemical characterization of produced oils and gases in immiscible and miscible CO_2 flooding processes. *Energy & Fuels*, *27*(1), 440-453.

(26) Zhou, X., Jiang, Q., Yuan, Q., Zhang, L., Feng, J., Chu, B., ... & Zhu, G.,2020. Determining CO_2 diffusion coefficient in heavy oil in bulk phase and in porous media using experimental and mathematical modeling methods. *Fuel*, *263*, 116205.

(27) Wang, S., Chen, S., & Li, Z.,2016. Characterization of produced and residual oils in the CO_2 flooding process. *Energy & Fuels*, *30*(1), 54-62.

(28) Honarpour, M.M., Nagarajan, N.R., Grijalba Cuenca, A., Valle, M. and Adesoye, K., 2010, January. Rock-fluid characterization for miscible CO_2 injection: residual oil zone, Seminole field, Permian Basin. In *SPE Annual Technical Conference and Exhibition*. Society of Petroleum Engineers.

(29) Chang, C., Zhou, Q., Kneafsey, T.J., Oostrom, M., Wietsma, T.W. and Yu, Q., 2016. Pore-scale supercritical CO_2 dissolution and mass transfer under imbibition conditions. *Advances in Water Resources*, *92*, pp.142-158.

(30) Seyyedsar, S.M., Farzaneh, S.A. and Sohrabi, M., 2015, September. Enhanced heavy oil recovery by intermittent CO_2 injection. In *SPE Annual Technical Conference and Exhibition*. Society of Petroleum Engineers.

(31) Zanganeh, P., Dashti, H. and Ayatollahi, S., 2015. Visual investigation and modeling of asphaltene precipitation and deposition during CO_2 miscible injection into oil reservoirs. *Fuel*, *160*, pp.132-139.

(32) Okwen, R.T., 2006, January. Formation Damage by CO_2 Asphaltene Precipitation. In *SPE International Symposium and Exhibition on Formation damage control*. Society of Petroleum Engineers.

(33) Li, X., Chi, P., Guo, X. and Sun, Q., 2019. CO_2-induced asphaltene deposition and wettability alteration on a pore interior surface. *Fuel*, *254*, p.115595.

(34) Glover, P.W.J. and Walker, E., 2008. Grain-size to effective pore-size transformation derived from electrokinetic theory. *Geophysics*, 74(1), pp. E17-E29.

(35) Zou, Y., Li, S., Ma, X., Zhang, S., Li, N. and Chen, M., 2018. Effects of CO_2–brine–rock interaction on porosity/permeability and mechanical properties during supercritical-CO_2 fracturing in shale reservoirs. *Journal of Natural Gas Science and Engineering*, *49*, pp.157-168.

(36) Wang, C., Li, T., Gao, H., Zhao, J. and Gao, Y., 2018. Quantitative study on the blockage degree of pores due to asphaltene precipitation in low-permeability reservoirs with NMR technique. *Journal of Petroleum Science and Engineering*, *163*, pp.703-711.